FINNISH METEOROLOGICAL INSTITUTE
CONTRIBUTIONS

NO. 146

# MODELLING OF ARCTIC STRATOSPHERIC OZONE AND WATER VAPOUR AND THEIR CHANGES

Laura Thölix

Department of Physics
Faculty of Science
University of Helsinki
Helsinki, Finland

ACADEMIC DISSERTATION in meteorology

To be presented, with permission of the Faculty os Science of the University of Helsinki, for public criticism in Auditorium Physicum E204 (Gustaf Hällströmin katu 2b) on November 6th, 2018, at 12 o'clock noon.

Finnish Meteorological Institute
Helsinki, 2018

Supervisors Dr. Leif Backman
Climate System Research
Finnish Meteorological Institute, Helsinki, Finland

Research prof. Alexey Karpechko
Meteorological Research
Finnish Meteorological Institute, Helsinki, Finland

Pre-examiners Dr. rer. nat. Farahnaz Khosrawi
Institute for Meteorology and Climate Research
Karlsruhe Institute of Technology, Karlsruhe, Germany

Dr. Olaf Morgenstern
Climate Variability and Change Programme
National Institute of Water and Atmospheric Research Ltd,
Wellington, New Zealand

Opponent Prof. Ilona Riipinen
Department of Environmental Science and Analytical Chemistry
Stockholm University, Stockholm, Sweden

Custos Prof. Heikki Järvinen
Department of Physics
University of Helsinki, Helsinki, Finland

ISBN 978-952-336-057-0 (paperback)
ISBN 978-952-336-058-7 (pdf)
ISSN 0782-6117

Erweko
Helsinki, 2018

FINNISH METEOROLOGICAL INSTITUTE

Published by
Finnish Meteorological Institute
(Erik Palménin aukio 1) , P.O. Box 503
FIN-00101 Helsinki, Finland

Series title, number and report code of publication
Finnish Meteorological Institute
Contributions 146, FMI-CONT-146

Date
October 2018

Author
Laura Thölix

Title
Modelling of Arctic stratospheric ozone and water vapour and their changes

Abstract

Ozone and water vapour are important trace gases in the atmosphere, where both play an important role in radiative and chemical processes. Ozone protects the Earth's biosphere, humans and materials from the harmful ultraviolet (UV) radiation. The distributions and changes of ozone and water vapour are thus important to understand. Restrictions on the production and use of ozone depleting substances (ODS) within the Montreal Protocol have stopped the growth of the ozone loss, even signs of recovery of the ozone layer have been seen. However, many ODSs are long lived in the atmosphere and it will take decades before they are removed. Stratospheric water vapour influences the polar ozone loss by controlling the formation of polar stratospheric clouds (PSC). The climate change will cool the stratosphere, which could favour the formation of PSCs. This could cause significant ozone depletion despite the lower chlorine loadings in the future stratosphere. Atmospheric models are needed for studying these phenomena, because the number of observations is limited. Also the prediction of future ozone loss requires models.

In this study simulations of the middle atmosphere have been made using the FinROSE chemistry transport model (FinROSE-CTM). It is an off-line 3-dimensional model, covering the altitude range of ca. 10−80 km, including the stratosphere. The model can be used for short term case studies, as well as for decadal simulations. The FinROSE-CTM needs pre-calculated winds, temperature and surface pressure, and then calculates the chemistry and transport using the meteorology. In this study ECMWF reanalysis data and climate model data have been used. Model results have been compared to ground based and satellite observations, and the model has been shown to be suitable for polar stratospheric ozone and water vapour studies. When running the model with climate model data also future conditions can be predicted.

Both observations and simulations show an increase in the water vapour concentration in the Arctic stratosphere after 2006, but around 2012 the concentration started to decrease. Model calculations suggest that this increase in water vapour is mostly explained by transport-related processes. The increase in water vapour in the presence of the low winter temperatures in the Arctic stratosphere led to more frequent occurrence of ICE PSCs in the Arctic vortex. In a recent study, we studied the effect of changes in the water vapour concentration in the tropical tropopause on Arctic ozone depletion. A change in the tropical tropopause water vapour concentration resulted in a corresponding change in the Arctic stratosphere. We found that the impact of water vapour changes on ozone loss in the Arctic polar vortex depends on the meteorological conditions. The strongest effect was in intermediately cold conditions, when added water vapour resulted in more ozone loss due to the additional PSCs and associated chlorine activation on their surface. The effect was less pronounced in cold winters because cold conditions persisted long enough for a nearly complete chlorine activation even with observed water vapour. The results show that the simulated water vapour concentration in the tropical tropopause has a significant impact on the Arctic ozone loss and deserves attention, and therefore needs to be well simulated in order to improve future projections of ozone layer recovery.

Publishing unit
Finnish Meteorological Institute

Classification (UDC)
551.5
551.510.532
551.510.534

Keywords
ozone, water vapour, stratosphere, polar vortex, chemsiry-transport model

ISSN and series title
0782-6117 Finnish Meteorological Institute Contributions

ISBN
978-952-336-057-0 (paperback), 978-952-336-058-7 (pdf)

Language
English

Pages
132

ILMATIETEEN LAITOS

Julkaisija
Ilmatieteen laitos
(Erik Palménin aukio 1)
PL 503, 00101 Helsinki

Julkaisun sarja, numero ja raporttikoodi
Finnish Mereorological Institute
Contributions 146, FMI-CONT-146

Julkaisuaika
Lokakuu 2018

Tekijä
Laura Thölix

Nimike
Arktisen stratosfäärin otsonin ja vesihöyryn sekä niiden muutosten mallintaminen

Tiivistelmä

Otsoni ja vesihöyry ovat tärkeitä hivenkaasuja ilmakehässä. Vesihöyry on yksi merkittävimmistä kasvihuonekaasuista, sillä se vaikuttaa maapallon säteilytasapainoon sekä moniin kemiallisiin reaktioihin ilmakehässä. Otsoni sen sijaan suojaa ihmisiä ja luontoa haitalliselta ultravioletisäteilyltä. Sekä vesihöyryn että otsonin jakauma sekä niiden pitoisuuksien muutokset nykyisessä ja tulevaisuuden ilmakehässä ovat tärkeitä ymmärtää. Vaikka Montrealin protokollan asettamat rajoitukset otsonia tuhoavien CFC-kaasujen valmistukselle ja käytölle ovat saaneet otsonikerroksen tuhoutumisen pysähtymään, kestää otsonikerroksen palautumisessa ennalleen vielä pitkään. Ilmastonmuutos jäähdyttää stratosfääriä, jolloin polaaristratosfääripilvet (PSC) voivat lisääntyä, ja otsonia voi tulevaisuudessa tuhoutua enemmän, vaikka kloorin määrä ilmakehässä onkin pienempi. Näiden asioiden tutkimiseen tarvitaan ilmakehämalleja, sillä havaintoja stratosfääristä on rajoitetusti, eikä niitä myöskään ole tulevaisuuden ilmastosta.

Tässä tutkimuksessa on stratosfäärin olosuhteiden tutkimiseen käytetty FinROSE kemiakuljetusmallia. Malli on globaali ja se kattaa stratosfäärin eli korkeusvälin 10-80 km. Mallilla voidaan tehdä sekä lyhyitä tapaustutkimuksia että pitkiä, vuosikymmeniä kattavia simulaatioita. Malli tarvitsee syötteeksi meteorologista dataa: tuulet, lämpötilat ja pintapaineen. Tässä tutkimuksessa mallia on ajettu käyttäen ECMWF:n analyysejä tai ilmastomallilla etukäteen laskettua meteorologiaa. Lähtötiedon vaikutusta mallin antamiin tuloksiin tutkittiin, ja havaittiin sillä olevan suuri merkitys tulosten luotettavuuteen. FinROSE:lla laskettuja otsoni- ja vesihöyrypitoisuuksia verrattiin sekä satelliitti- että maanpintahavaintoihin, ja mallin todettiin tuottavan käyttökelpoisia tutkimustuloksia. Ilmastomallin meteorologialla FinROSE:a ajettaessa on ollut mahdollista tehdä ennusteita myös tulevaisuuden otsonikadoista.

Tutkimuksen tuloksena selvisi, että vesihöyry on lisääntynyt stratosfäärissä vuosina 2006-2012, mutta 2012 jälkeen pitoisuus on vähentynyt. Mallisimulaatiot osoittavat, että veden lisäys johtuu pääosin kuljetuksesta; enemmän vettä on kulkeutunut tropiikista navoille. Ilmastonmuutoksen vuoksi kylmenevässä stratosfäärissä kosteassa ilmassa arktisilla polaarialueilla voi muodostua entistä enemmän polaaristratosfääripilviä (PSC), joiden pinnalla klooriyhdisteet tuhoavat otsonia katalyyttisesti. Viimeisin tutkimus osoitti, että vesihöyry vaikuttaa otsonikatoon arktisella alueella eri tavoin erilaisissa meteorologisissa olosuhteissa. Suurin vaikutus on kohtalaisen kylminä talvina, jolloin veden lisäys lisäsi otsonikatoa selvästi. Tämä johtui lisääntyneistä polaaripilvistä ja klooriaktivaatiosta. Kylminä talvina vaikutus jäi vähäisemmäksi, sillä klooriaktivaatio oli silloin lähes täydellinen havaintoihin perustuvallakin vesihöyrymäärällä. Tulokset osoittavat, että tropiikin tropopaussin vesihöyryn määrällä on vaikutusta arktiseen otsonikatoon, ja että se on mallinnettava ilmastomalleissa oikein, että otsonikato voidaan ennustaa oikein.

Julkaisijayksikkö
Ilmatieteen laitos

Luokitus (UDK)
551.5
551.510.532
551.510.534

Asiasanat
otsoni, vesihöyry, stratosfääri, polaaripyörre, kemiakuljetusmalli

ISSN ja avainnimike
0782-6117 Finnish Meteorological Institute Contributions

ISBN
978-952-336-057-0 (nid.), 978-952-336-058-7 (pdf)

Kieli
englanti

Sivumäärä
132

# PREFACE

This work was carried out at the Finnish Meteorological Institute (FMI) in groups and units whose names have changed over the years following the various organization changes. This work was mainly funded by the Academy of Finland and the EC. It has taken a long time to finish the thesis and during all these years I have had opportunity to work with many nice and bright persons. There have been so many people who have impact this work, that I cannot name them all.

I would like to thank FMI, the management and all my former and current foremen for the excellent working conditions and all the help and support. They all have shown interest in my work and trust me. I have had possibility to continue this work regardless of changing founding situations. I am also grateful to Dr Farahnaz Khosraw from Karlsruhe Institute of Technology and Dr Olaf Morgenstern from National Institute of Water and Atmospheric Research Ltd, Wellington for reviewing the thesis, for prof. Heikki Jrvinen from University of Helsinki for acting as a custos and for prof. Ilona Riipinen from Stockholm University for accepting to be my opponent.

The greatest thanks belongs to co-authors. Especially I want to thank my colleague and supervisor Leif Backman. Together we have tried to solve modelling problems during these years. I could always have trust Lefa's knowledge and understanding of atmospheric chemistry. I don't think this thesis would have been finished without his help. Warm thanks belongs also to my other supervisor Alexey Karpechko, who has provided important help and support in interpreting of the results and writing of the papers. Thanks also my former supervisor and current director general of FMI Juhani Damski who familiarized me with the FinROSE model. Thanks my colleague Rigel Kivi, who was leading the project where the two latest papers were started. In addition, I would like to thank Petteri Taalas, who initiated this work by employing me to the Ozone and UV radiation research group, was my first supervisor and promised that defending thesis in Finnish is possible.

Years at FMI have been nice, when I have had wonderful people around me. Thanks for the company and great discussions during the lunch breaks Outi, Anu and Lefa. Thanks all the people in the 3rd floor coffee table for nice atmosphere. Thanks Sanna for our long work and no-work related discussions, which I have already missed. Thanks especially Kaisa for support and motivation of me during all these years. You all have meant a lot to me.

Finally I want to thank my lovely neighbors, other friends, parents and family Mika and Linnea. Thanks that you preset!

Helsinki, October 2018
Laura Thölix

# CONTENTS

## ABBREVIATIONS

| | |
|---|---|
| AGAGE | Advanced Global Atmospheric Gases Experiment |
| BD | Brewer–Dobson |
| CALIPSO | Cloud-Aerosol-Lidar and Infrared Pathfinder Satellite Observations |
| CCM | Chemisrty coupled climate model |
| CTM | Chemistry–transport model |
| CFC | Chloro-fluoro-carbon |
| DU | Dobson unit |
| ECMWF | European Centre for Medium-range Weather Forecasts |
| ERA | ECMWF Re-analysis |
| GOME | Global Ozone Monitoring Experiment |
| HCFC | Hydrochlorofluorocarbon |
| MLS | Microwave Limb Sounder |
| NAT | Nitric Acid Trihydrate |
| ODS | Ozone depleting substances |
| OMI | Ozone Monitoring Instrument |
| PSC | Polar stratospheric clouds |
| PV | Potential vorticity |
| PVU | Potential vorticity unit |
| QBO | Quasi-Biennial-Oscillation |
| SCIAMACHY | Scanning Imaging Absorption Spectrometer for Atmospheric |
| STS | Supercooled Ternary Solutions |
| SWV | Stratospheric vater vapour |
| TOMS | Total Ozone Mapping Spectrometer |
| UMETRAC | Unified Model with Eulerian Transport and Chemistry |
| UTLS | Upper troposphere lower stratosphere |
| UV | Ultraviolet |

# LIST OF ORIGINAL PUBLICATIONS

I Damski, J., Thölix, L., Backman, L., Taalas, P., and Kulmala, M.: FinROSE — middle atmospheric chemistry and transport model, *Boreal Environ. Res.*, **12**, 535–550, 2007.

II Thölix, L., Backman, L., Ojanen, S.-M.: The effects of driver data on the performance of the FinROSE chemistry transport model, *IJRS*, **31**, 6401–6408, 2010.

III Damski, J., Thölix, L., Backman, L., Kaurola, J., Taalas, P., Austin, J., Butchart, N., Kulmala, M.: A chemistry–transport model simulation of middle atmospheric ozone from 1980 to 2019 using coupled chemistry GCM winds and temperatures, *Atmos. Chem. Phys.*, **7**, 2165–2181, 2007.

IV Thölix, L., Backman, L., Kivi, R., and Karpechko, A. Yu.: Variability of water vapour in the Arctic stratosphere, *Atmos. Chem. Phys.*, **16**, 4307–4321, 2016.

V Thölix, L., Karpechko, A.Yu., Backman, L. and Kivi, R.: Linking the uncertainty in simulated Arctic ozone losses to modelling of tropical stratospheric water vapour, *Atmos. Chem. Phys. Discuss.*, in review, 2018.

In PAPER II, IV and V L. Thölix was responsible for the model development and calculations and major part of the analysis of the results as well as the writing of the manuscripts. In PAPER I and III L. Thölix contributed to the model development, carried out the FinROSE simulations, was involved in the interpretation of results and contributed to writing the manuscripts.

# 1 INTRODUCTION

Most atmospheric ozone is in the stratosphere, between 15 and 35 km. This layer is called the ozone layer and it protects the Earth's biosphere, humans and materials from harmful ultraviolet (UV) radiation. Already in the 1970's scientists noticed, that anthropogenic Chlorofluorocarbon (CFC) compounds have the potential to destroy ozone (Molina and Rowland, 1974). In 1985 a massive decrease in ozone (the ozone hole) was observed during the Antarctic spring (Farman et al., 1985), and chlorine and bromine compounds in the CFCs were found to have caused it (Solomon et al., 1986; WMO, 2014). Research activity on the stratosphere and the ozone layer increased and quick political action was taken. This led to the Montreal Protocol on Substances that Deplete the Ozone Layer, which was agreed on in 1987. The protocol regulates and slows down the use and production of Ozone-depleting substances (ODSs). It is the most extensive environmental agreement, and all the countries in the world have ratified it. In the industrialized countries production of CFCs was banned in 1996 and in 2010 also worldwide. The protocol has been amended a few times afterwards. The Montreal Protocol has been a success story in international environmental protection. The amounts of ODSs in the atmosphere have decreased. The concentration of tropospheric chlorine reached its peak value in 1993 and tropospheric bromine a little later, in 1997. The amount of stratospheric chlorine follows the tropospheric ODS; however, there is a lag, because its transport in the stratosphere is slow (Newman et al., 2007). And although the impact to the ozone levels is more difficult to detect, the ozone layer is recovering (WMO, 2014; Solomon et al., 2016; Chipperfield et al, 2017; Strahan and Douglass, 2018). ODSs are also greenhouse gases, so the reduction of CFCs has also helped to mitigate climate change.

Climate change is expected to affect the temperature distribution in the atmosphere. The troposphere is warming, while the stratosphere is cooling with increasing carbon dioxide ($CO_2$) loadings (Fleming et al., 2011), up to now this cooling has been about 0.5 K/decade. $CO_2$ changes will also change stratospheric circulation which is expected to change ozone distribution (see Section 2.5). Stratospheric concentrations of other greenhouse gases, like nitrous oxide ($N_2O$) and methane ($CH_4$) that are transported from the troposphere to the stratosphere, will increase. These gases have an effect on the climate by changing the radiative circumstances, and in addition they affect ozone chemistry (Fleming et al., 2011; Stolarksi et al., 2015). For example an increase in methane would increase water vapour (SWV) and other $HO_x$ compounds in the stratosphere, which changes both the radiation balance and ozone chemistry (Dvortsov and Solomon, 2001; Eyring et al., 2013). $N_2O$ is the main source of $NO_x$, which is one of the most important ozone destructors (Ravishankar et al., 2009).

Water vapour is a minor constituent in the stratosphere. The concentration is typ-

ically about 3–6 v (e.g., Randel et al., 2004). However, $H_2O$ has an important role in radiative and chemical processes. In the upper troposphere/lower stratosphere (UTLS) changes in the water vapour concentration result in significant changes in the radiative forcing of the atmosphere (Riese et al., 2012). Odd hydrogen $HOx$, which forms during the photodissociation of SWV, contributes to the chemical ozone loss in the catalytic cycles of the stratosphere (Dvortsov and Solomon, 2001). SWV can intensify ozone destruction also by forming polar stratospheric clouds (PSCs), when the temperature drops low enough (Khosrawi et al., 2016). PSCs enable the conversion of inert halogen reservoir species to active halogen radicals (e.g., Solomon, 1999). Heterogeneous reactions on the surfaces of PSC particles can lead to massive ozone depletion inside polar vortex, when the atmospheric concentration of halogens is sufficiently high (Solomon et al., 2014; McElroy et al., 1986; Wohltmann et al., 2013; Thölix et al., 2016; Khosrawi et al., 2017; Thölix et al., 2018).

Atmospheric ozone is observed from the ground as well as from satellites. From the ground both in-situ, e.g. soundings, and remote sensing methods, e.g. Dobson and Brewer spectrometers can be used to observe atmospheric ozone concentrations. Ground based observations, however, describe only the local ozone situation. Satellite observations on the other hand give the global ozone distribution. Observations provide valuable information about the situation of the atmosphere, but also models are needed. With the help of models we can understand the mechanisms in the atmosphere. Ozone can be modelled with chemistry–transport models (CTM) as well as with the chemistry coupled climate models (CCM). CCMs are needed for future scenarios, while CTMs driven by meteorological reanalysis data are good tools for a variety of case-studies, because the results obtained can be compared to observations. Computational requirements are typically lower for the CTMs compared to CCMs.

The amount of ozone in the Arctic varies considerably from one year to another because of atmospheric circulation variability. The size of Arctic ozone losses varies a lot between years, and no clear trend can be seen in them (WMO, 2014). Increasing SWV could lead to an increasing PSC volume trend, which has already been seen in the lower Arctic stratosphere (Khosrawi et al., 2016; Thölix et al., 2016). The Arctic ozone loss is very dependent on the conditions in the polar vortex, i.e. significant losses have been observed in cold winters, but when the polar vortex has been weak, the ozone losses have remained small (Rex et al., 2006; Müller et al., 2008; Manney et al., 2011; Solomon et al., 2014; Chipperfield et al., 2015; Thölix et al., 2016).

Motivated by the variability of Arctic ozone loss, the work done for this thesis was aimed at studying the distribution and long term changes of stratospheric ozone and water vapour in the Arctic. The results concentrate on the effect of the increase in stratospheric water vapour on PSC occurrence, and the quantified impact of tropical water vapour on Arctic ozone losses. The model simulations have been done by

using FinROSE-CTM, which is also validated during this work. First I will describe the model and after that I will describe the research done with the model. The study includes the following papers:

- (PAPER I) describes the FinROSE chemistry transport model and shows its capability of simulating a realistic distribution of stratospheric ozone from seasonal to decadal scales, by comparing the model results to the observations.
- (PAPER II) discusses the quality and properties of the driver data and the effects of them on the chemistry transport model simulations and model results.
- (PAPER III) describes the trends and variability of ozone between 1980 and 2019. It also shows that it is possible to use FinROSE driven by a climate model to simulate future years.
- (PAPER IV) describes the water vapour distribution in the Arctic stratosphere. It aims to show long term changes in the stratospheric water vapour distribution and the sources of the changes.
- (PAPER V) considers the importance of water vapour for the Arctic ozone loss in different dynamical conditions. It describes how the changes in the stratospheric water vapour concentration affect the ozone depletion in the Arctic stratosphere.

The introductory part of this thesis is organised as follows: Chapter 2 gives an introduction to stratospheric chemistry and dynamics, especially concerning ozone loss and the effect of water vapour. Chapter 3 represents the materials and methods, ie. model and data, and PAPER I. Chapter 4 presented the main results from PAPERS I – V. Conclusions are drawn in Chapter 5.

# 2 STRATOSPHERIC CHEMISTRY AND DYNAMICS

The ozone layer is located in the stratosphere at an altitude of 15–35 km. There it absorbs solar radiation, especially at the UV radiation wavelengths, and prevents the harmful UV radiation from reaching the Earth's surface. Our current life on earth would not be possible without the ozone layer. In addition, because ozone absorbs solar radiation it is important for the temperature profile of the stratosphere. In the atmosphere there is on average 300 DU ozone. One Dobson unit (DU) represents a 0.01 mm thick layer of ozone under near-surface conditions, i.e. 300 DU ozone thus corresponds to a three mm layer.

The most important phenomenon in the stratospheric general circulation at high latitudes in winter is the polar vortex. In the local autumn, especially in the southern hemisphere, the temperature difference between the tropics and the polar region grows considerably because of the decrease in solar irradiance. The air mass in the polar area cools quickly and the temperature gradient grows. This will cause a strong westerly wind, which isolates the Antarctic polar region from the mid-latitude air. This polar vortex is stable and cold. Also a polar vortex forms in the autumn in the Arctic. The northern vortex is not as stable, cold and long-lasting as the southern hemisphere one because of the different land-sea distribution and the topography. However, in both of the vortices polar stratospheric clouds can form, where reactions that lead to effective ozone depletion, can take place.

## 2.1 CHAPMAN CHEMISTRY

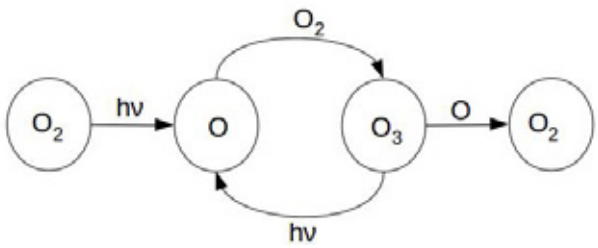


FIGURE 2.1. A schematic of the Chapman mechanism, where UV radiation initiates ozone formation and dissociates the ozone molecule.

The production rate of ozone is the highest in the tropics and mid-latitudes from oxygen photodissociation. In this process, the UV radiation splits an oxygen molecule into two oxygen atoms, which react quickly with other oxygen molecules to form ozone. However, ozone molecules also absorb solar radiation and break into an oxygen atom and an oxygen molecule, thus being destroyed ozone. Oxygen is rapidly cycled between $O$ and $O_3$ and therefore it is convenient to use the sum of them: odd oxygen ($O_x$ = $O$ + $O_3$). Natural ozone production and destruction is known as the Chapman cycle (Chapman, 1930), and a simplified illustration of the cycle is shown in Fig. 2.1. Photochemical dissociation of oxygen (eq. (2.1)) is fast in the upper stratosphere and mesosphere, where solar radiation is strong. In the lower and middle stratosphere it is a slow process. However, the resulting ozone formation (eq. (2.2)) is fast, as well as the photochemical dissociation (eq. (2.3)). In reaction (2.3) ozone absorbs ultraviolet radiation, and simultaneously prevents the propagation of UV radiation to the Earth's surface. In the absorption the released energy warms the stratosphere and is the cause of the temperature distribution in the stratosphere, where the temperature rises. Ozone destruction by reaction with an oxygen atom (eq. (2.4)), on the other hand, is slow. The decrease of odd oxygen means there is ozone loss.

$$O_2 + h\nu(\lambda \leq 242\,nm) \rightarrow 2O \tag{2.1}$$

$$O + O_2 + M \rightarrow O_3 + M \tag{2.2}$$

$$O_3 + h\nu(\lambda = 200 - 320\,nm) \rightarrow O + O_2 \tag{2.3}$$

$$O + O_3 \rightarrow 2O_2 \tag{2.4}$$

The Chapman chemistry would produce an ozone distribution with most of the ozone in the tropics, and very low ozone concentrations in the polar regions, not in line with the observed distribution of ozone in the atmosphere. In addition to the Chapman chemistry the atmospheric circulation, see Section 2.5, is essential for understanding the observed ozone distribution. Furthermore, also $NO_x$ and $HO_x$ chemistry is needed to explain the natural ozone distribution. In polar areas the natural climatological ozone maximum occurs in the late winter and the minimum is observed in the early autumn. Low ozone values observed in the spring time polar vortex (ozone hole) cannot be explained by the processes described above.

## 2.2 CATALYTIC REACTIONS

In addition to the production and destruction of ozone by the Chapman cycle, the ozone levels are be determined by the catalytic reactions involving radicals (for example, Solomon (1999)). Those radicals can be odd hydrogen species ($HO_x = H +$

$OH + HO_2$), odd nitrogen species ($NO_x = NO + NO_2$), as well as halogen species (i.e. chlorine and bromine). In catalytic cycles ozone is destroyed very quickly and efficiently, for example one chlorine or bromine atom can destroy several thousand ozone molecules.

In the stratosphere the $NO_x$ is generated in the reaction (2.5):

$$N_2O + O(^1D) \rightarrow 2NO \tag{2.5}$$

$HO_x$ is produced mainly from water vapour (reaction (2.6)):

$$H_2O + O(^1D) \rightarrow 2OH \tag{2.6}$$

The general form of the catalytic ozone loss cycle is shown in eq. (2.7)-(2.9):

$$X + O_3 \rightarrow XO + O_2 \tag{2.7}$$

$$XO + O \rightarrow X + O_2 \tag{2.8}$$

$$Net : O + O_3 \rightarrow 2O_2 \tag{2.9}$$

where X is a catalyst that can be either $NO$ or $OH$. In this cycle one oxygen atom and one ozone molecule (two $O_x$) are depleted and two molecular oxygens are produced. The catalyst X stays unchanged, and can continue to destroy ozone. $NO_x$ is a more important catalyst in the stratosphere, while $HO_x$ works effectively higher in the mesosphere.

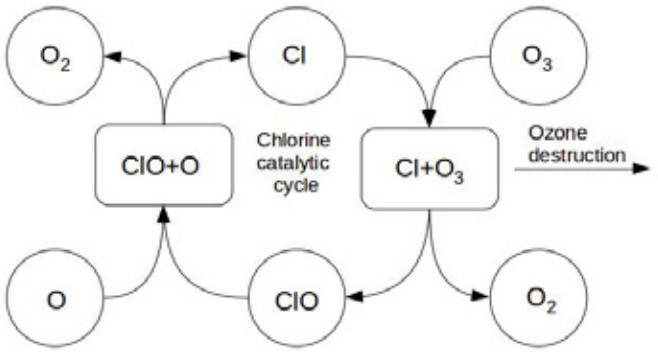


FIGURE 2.2. Catalytic chlorine cycle. The figure is modified from Fahey and Heglin (2011).

Due to human activities ODSs, such as CFCs, hydrochlorofluorocarbon (HCFCs) and other chlorine and bromine containing compounds been released into the atmosphere (for example WMO (2014)). These gases are very long-lived in the troposphere, and dissociate due to sunlight only after being transported to the stratosphere by atmospheric circulation. Released chlorine and bromine radicals participate in the catalytic ozone destruction cycle, this is illustrated in Fig. 2.2 and also in the equations eq. (2.10)-(2.12):

$$Cl + O_3 \rightarrow ClO + O_2 \tag{2.10}$$

$$ClO + O \rightarrow Cl + O_2 \tag{2.11}$$

---

$$Net : O_3 + O \rightarrow 2O_2 \tag{2.12}$$

At lower altitudes in the stratosphere the concentration of oxygen atoms is low, therefore these processes are not efficient. Neither the Chapman mechanism nor the reactions of eq. (2.10)-(2.12) could explain the formation of the ozone hole. Laboratory experiments showed that the following catalytic cycles (eq. (2.13)-(2.20)) are involved in the polar ozone loss (Molina and Molina, 1987; McElroy et al., 1986):

Cycle 1:

$$ClO + ClO + M \rightarrow Cl_2O_2 + M \tag{2.13}$$

$$Cl_2O_2 + h\nu \rightarrow 2Cl + O_2 \tag{2.14}$$

$$2Cl + 2O_3 \rightarrow 2ClO + 2O_2 \tag{2.15}$$

---

$$net : 2O_3 \rightarrow 3O_2 \tag{2.16}$$

Cycle 2:

$$BrO + ClO \rightarrow Cl + Br + O_2 \tag{2.17}$$

$$Br + O_3 \rightarrow BrO + O_2 \tag{2.18}$$

$$Cl + O_3 \rightarrow ClO + O_2 \tag{2.19}$$

---

$$net : 2O_3 \rightarrow 3O_2 \tag{2.20}$$

Chlorine released from ODSs form so called reservoir species such as $HCl$ (hydrochloric acid) and $ClONO_2$ (chlorine nitrate), which do not cause ozone depletion ((2.21)–(2.22)). Similar reactions also occur in the case of bromine. Thus gas phase chemistry is not enough to explain the massive ozone depletion in the polar regions.

$$ClO + NO_2 \rightarrow ClONO_2 \tag{2.21}$$

$$Cl + CH_4 \rightarrow HCl + CH_3 \tag{2.22}$$

## 2.3 POLAR OZONE LOSS

In the cold conditions of the polar vortex PSCs are formed. PSCs typically consist of sulphuric acid ($H_2SO_4$), nitric acid ($HNO_3$) and water vapour ($H_2O$). PSCs are divided into two main types, I and II. Type I PSCs are further divided into two sub types, Ia and Ib. Type Ia, Nitric Acid Trihydrate (NAT), are solid and consist of nitric acid and water. Type Ib, Supercooled Ternary Solutions (STS), are liquid solutions of sulphuric acid, nitric acid and water. Type II PSCs consist of ice particles (ICE). For typical conditions at an altitude of about 20 km the threshold temperature for PSC formation is 195 K or -78° C for Type I and 188 K or -85° C for Type II (e.g. Carslaw et al., 1994). In the vortex of the southern hemisphere these temperatures are passed every winter, but in the northern hemisphere they are less common. Even though, conditions cold enough for the formation of PSCs occur in the north almost every winter the conditions often persist only for a short time and occur in a limited area. In some winters (1996/97, 1999/2000, 2004/05 and 2010/11) the cold conditions persisted also in the Arctic enabling significant ozone depletion (Solomon, 1999; WMO, 2014).

Heterogeneous reactions on PSCs are important in the ozone loss chemistry for converting the chlorine and bromine reservoir species to more active species. Eq. (2.23)–(2.28) show the heterogeneous reactions where halogen reservoir species react to form intermediate species (like $HOCl$, $Cl_2$, $BrCl$ and $HOBr$). In the cace of PSCs in the heterogeneous reactions one reactant is in the gas phase and the other is solid.

$$ClONO_2(g) + H_2O(s) \rightarrow HOCl(g) + HNO_3(s) \tag{2.23}$$

$$BrONO_2(g) + H_2O(s) \rightarrow HOBr(g) + HNO_3(s) \tag{2.24}$$

$$ClONO_2(g) + HCl(s) \rightarrow Cl_2(g) + HNO_3(s) \tag{2.25}$$

$$HOCl(g) + HCl(s) \rightarrow Cl_2(g) + H_2O(s) \tag{2.26}$$

$$BrONO_2(g) + HCl(s) \rightarrow BrCl(g) + HNO_3(s) \tag{2.27}$$

$$HOBr(g) + HCl(s) \rightarrow BrCl(g) + H_2O(s) \tag{2.28}$$

When sunlight reaches the polar vortex in the spring, the intermediate species will photodissociate to form radicals ($Cl$, $ClO$, $Br$, $BrO$). The chlorine and bromine

radicals will then catalyse the ozone depletion reactions (Eq. (2.13)–(2.20)). As spring advances the temperature increases and PSCs will no longer form. The active chlorine is then transformed back to reservoir species through reactions with methane (2.21) or nitrogen dioxide (2.22), which will stop the ozone depletion.

Sedimentation, the downward motion of atmospheric particles, can prolong the ozone loss (Fahey et al., 2001). Type I PSCs are small ($\sim$1 micron), and therefore they have very small sedimentation velocities ($\sim$10 metres per day). Whereas type II PSC particles can be greater than 10 microns, and can settle out of the stratosphere rapidly ($\sim$1.5 km/day). Sedimentation removes reactive nitrogen and water. The removal of reactive nitrogen is known as denitrification and the removal of water vapour is known as dehydration. Denitrification and dehydration can occur inside the polar vortex in cold winters, decreasing the removal rate of $ClO$ through reaction with $NO_2$ to form the reservoir $ClONO_2$ (e.g. NASA, 2000). Denitrification therefore prolongs the occurrence of high levels of active chlorine thus prolonging the ozone loss (see e.g. Rex et al. (1997)).

The southern polar vortex is strong, cold and isolated and the formation of PSCs is effective, with significant occurrence of ICE PSCs, effective halogen activation and strong sedimentation. This causes an almost complete ozone depletion within the 15–20 km altitude range. In the Arctic the polar vortex is warmer and the ozone depletion remains weaker, with a maximum of about 40% (Manney et al., 2011; Livesey et al., 2015). However, in winter 2011, at some altitudes the ozone depletion reached 70% (Manney et al., 2011).

## 2.4 WATER VAPOUR AND ITS IMPACT ON THE POLAR OZONE LOSS

The dry air in the atmosphere consists mainly of nitrogen $N_2$ (78.1%) and oxygen $O_2$ (20.9%). The rest is argon $Ar$ and trace constituents, such as carbon dioxide $CO_2$, ozone $O_3$, methane $CH_4$, various oxides of nitrogen $NO_x$, neon $Ne$, and helium $He$. The amount of water vapour is variable; on average about 1% at sea level, and 0.4% over the entire atmosphere. The tropospheric concentration of water vapour is important as it creates many of the observed weather features, like clouds, rain, snow and ice. The stratosphere is much drier, with about 4–5 ppmv (0.0004 to 0.0006%) water vapour, but it still has a significant role in the energy budget of the atmosphere (e.g., Randel et al., 2004). Water vapour absorbs and emits the infrared radiation from the surface, retaining the atmospheric warmth. In addition, it is important in the formation of aerosols and polar stratospheric clouds.

The main source of SWV is the transport through the tropical tropopause (Brewer, 1949). Also the methane oxidation process in the stratosphere is a source of water vapour. The cold conditions in the tropical tropopause causes water vapour to condense,

which leads to dehydration of the rising air masses. Thus only a small proportion of the water vapour can get through the tropopause into the stratosphere.

The amount of water vapour in the stratosphere affects the formation of PSCs in cold polar vortex. Therefore it has a significant effect on polar ozone depletion, by enhancing chlorine activation through the heterogeneous reactions on the surface of PSC particles.

## 2.5 Dynamics and transport

Understanding atmospheric transport is important for the modelling and forecasting of ozone distribution. Ozone forms mainly in the tropics in the photodissociation reaction of oxygen (Eq. (2.1)). From there, it is transported towards the mid latitudes and poles, where the air masses descend. This circular motion is called the Brewer–Dobson-circulation (BD) (Butchart, 2014). The same motion also carries other long-lived gases (water, methane, nitrogen oxides and ODSs) from the tropics towards the poles. It takes about 4–5 years for an air parcel to be transported from the tropical tropopause to the polar vortex, because the vertical movement is very slow. In the tropical lower stratosphere the air is quite young, i.e. the age of the air is low. However, in the middle- and high-latitudes the age of the air can be 5 years. In the older air there is more inorganic chlorine and less CFCs, because the chlorine compounds have been exposed to UV radiation for a longer time, and are decomposed to reactive radicals. Figure 2.3 shows the seasonally averaged ozone distribution and the BD-circulation. Ozone is transported from its origin in the tropics to the winter pole, where its life time is long, because the amount of UV radiation is considerably lower there than in the tropics, and ozone is not destroyed photochemically.

The Brewer–Dobson-circulation is caused by planetary waves, which are generated by large scale topography and meridional temperature differences. Planetary waves, known also as Rossby waves, have horizontal wavelength up to 20000 km and move slowly westward, with respect to the zonal flow. They are also able to propagate vertically to the stratosphere (NASA, 2000). In the northern hemisphere there are much more differences in the geography (for instance the Rocky mountains and the Himalayas) and land-sea distribution than in the southern hemisphere. Thus wave energy is significantly larger in the northern stratosphere than in the southern stratosphere. This stronger wave activity in the northern hemisphere leads to a stronger BD-circulation in northern winters. More ozone is thus transported to the northern than to the southern high latitudes (NASA, 2000). The weaker winter wave activity in the southern hemisphere leads to a more isolated and colder Antarctic polar vortex compared to the Arctic one.

Also other dynamical waves affect the ozone distribution. One is the Quasi-Biennial Oscillation (QBO), which is a periodic east-west wind system in the tropics. It affects the year-to-year variability in the ozone distribution by modifying the temperature structure of the stratosphere and by modifying the BD-circulation. The QBO effect on water vapour is discussed in Section 4.4.

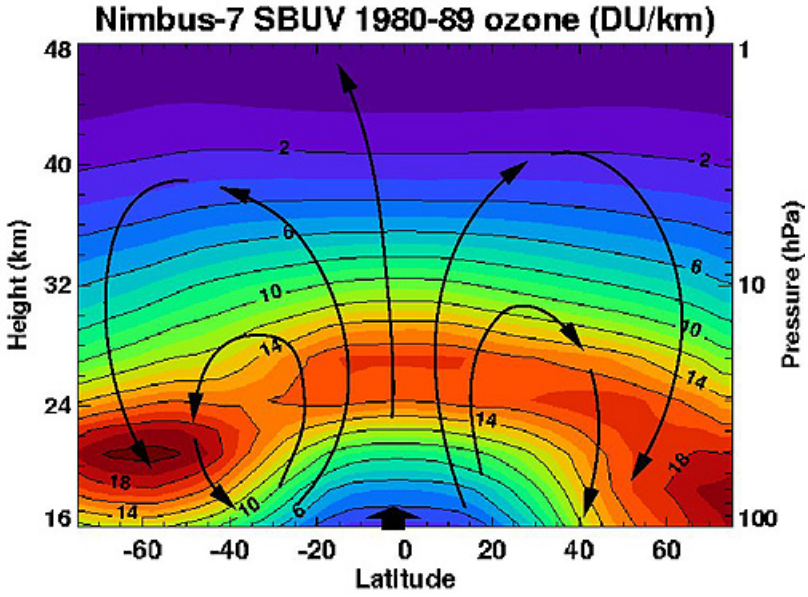


FIGURE 2.3. Brewer–Dobson circulation (arrows) and seasonally averaged ozone density (colours). From NASA (2000).

# 3 MODELLING AND DATA

This chapter describes the chemistry transport model FinROSE-CTM used in Section 3.1 and data used for modelling boundary and initial conditions. The validation of the model is presented in Section 3.2.

## 3.1 FINROSE-CTM

FinROSE is a global three-dimensional chemical transport model (Damski et al., 2007). Originally it is developed as the mechanistic general circulation model ROSE, and stratospheric chemistry was included afterwards (Rose and Brasseur, 1989). Later it was redesigned to be an off-line chemistry transport model. Off-line means that it does not calculate meteorological parameters by itself, but gets the needed temperatures, winds and surface pressure fields pre-calculated from some climate or weather prediction model. PAPER I presents the model in detail and describes the reforms that have been made in FMI. PAPER I presents the chemistry, where short-lived compounds are treated as families (Rose and Brasseur, 1989). In the family-concept fast-reacting compounds (like odd-oxygen: $O_x$ = $O(^3P)$, $O_3$ and $O(^1D)$) are grouped into longer lived chemical families, with lifetimes longer than the time step of the model, and they can be transported along the winds. After publishing PAPER I, the chemistry scheme was replaced by an other one, where the reaction rates of short-lived compounds also are calculated, the family approach is used only for transport. Also the heterogeneous chemistry scheme has been reformulated at FMI and is described in PAPER I. Boundary conditions are used for the troposphere and ion chemistry, this is only relevant in the mesosphere and is not taken into account in this model version.

A flux form semi Lagrangian transport method has been implemented at FMI. This method (Lin and Rood, 1996) solves the three-dimensional transport of volume mixing ratio fields, and better conserves the mass. In the horizontal direction the method of transport is a piecewise parabolic method (Colella and Woodward, 1984) and the vertical transport is calculated using the full monotonicity constraint (Lin and Rood, 1996). The vertical velocities are calculated internally from the continuity equation. Due to a somewhat too fast BD-circulation produced by the transport scheme with the used driver data, we nudge some long-lived tracers such as $N_2O$, $CH_4$ and total nitrogen $NO_y$ towards observations (see Section 3.2).

The concentrations of short- and long-lived chemical species, in the model, is solved by different schemes. The concentrations of short-lived gases ($O_3$, $O$, $H$, $OH$, $Cl$, $ClO$, $HO_2$, $N$, $NO$, $NO_2$, $Br$, $BrO$) are solved by the fully-implicit backward Euler system of nonlinear equations using the Newton–Raphson iteration. The chem-

istry of long-lived compounds is resolved by the Gauss–Seidel method by calculating the production and destruction rates, and then calculating a new concentration in each time step. The main reactions of ozone chemistry were presented in Chapter 2.

Photodissociation coefficients have been calculated with the PHODIS radiative transfer model (Kylling et al., 1995). Running the radiative transfer model in run-time in FinROSE's grid and time-step may be too expensive due to the CPU-intensive calculations. Instead coefficients were calculated in advance into look-up-tables. The photodissociation coefficient is then obtained by interpolating the tables based on altitude, solar zenith angle, ozone amount and albedo. Look-up tables have been calculated separately for winter and summer, and for five different latitude bands. This was done to ensure the most appropriate state of atmosphere from the table could be done and thus to improve the accuracy of the photodissociation coefficient.

## 3.2 DATA

A chemistry–transport-model needs a good initial state in order to give reasonable results. The initial values of the FinROSE simulations are usually from some previous run. If the concentrations in the model are in balance, there is no need for a separate spin-up, but if the model state is displaced a lot, a spin-up run has to be done first. Because atmospheric circulation is slow, the spin-up run has to be longer than the age-of-air, i.e. at least five years.

The tropospheric chemistry and emissions of the trace gases in the FinROSE-CTM are replaced with boundary conditions. Nudging towards the observed values of some long lived species helps to keep the stratospheric concentrations more in-line with observations in longer simulations. Ozone and water vapour values can be obtained from the driver data, usually from the ERA-Interim data. Data for long-lived species are derived from observations. A climatology calculated from the Microwave Limb Sounder (MLS) satellite observations is used as an upper boundary of ozone and water vapour. Tropospheric $N_2O$ data is from the Advanced Global Atmospheric Gases Experiment (AGAGE) (Prinn et al., 2000). In addition, the halogen loading for the troposphere ($Cl_y$ and $Br_y$) were obtained from updated Montzka et al. (2009) data. The model does not simulate the distribution of halogen source gases, but the stratospheric inorganic halogen loading is obtained by scaling the tropospheric $Cl_y$ and $Br_y$ with the age-of-air of the model. The carbon dioxide ($CO_2$) concentration is based on the global annual mean trend data (ftp://aftp.cmdl.noaa.gov/products/trends/co2). The concentration of the tropospheric methane ($CH_4$) is from the Global view-data (http://www.esrl.noaa.gov/gmd/ccgg/globalview/ch4).

The model is run by using pre-calculated winds and temperatures as a driver. FinROSE can be run with gridded meteorological data, and usually ECMWF ERA-Interim data is used (Dee et al., 2011). Driver data options and their impact on the results is the topic of PAPER III and is described in Chapter 4 of this thesis.

The results from FinROSE-CTM (mainly ozone and water vapour) have been validated in various projects against satellite observations and soundings. The results of the model validation have been reported in PAPER I and in Section 4.1. There the total ozone of FinROSE has been compared to the ECMWF ERA-40 data and the Total Ozone Mapping Spectrometer (TOMS) satellite ozone observations, as well as to ozone soundings. Already at the time of writing PAPER I, the results of FinROSE were comparable to observations, and the model provided improved ozone values compared to the driver data. Although the modelled ozone level showed a negative bias and the changes have been too smooth, the trend and the annual variation are described well. FinROSE-CTM has proven to be capable of simulating a realistic evolution of stratospheric ozone on seasonal to decadal scales.

# 4 RESULTS

In the following sections, the main results of this thesis are covered. The results of PAPERs I, II, III, IV and V are discussed in the following sections 4.1, 4.2, 4.3, 4.4 and 4.5, respectively.

## 4.1 FINROSE-CTM

The FinROSE model can be used to make both long simulations and shorter case studies. The model results were reasonable already at the time of writing PAPER I, and the model has subsequently been developed further in many areas, which has further improved the results. Figure 4.1 is a replotted Figure 5 from PAPER I. It is based on a later model version and the data is from a particularly strong ozone depletion year, 2011. The Figure shows the total column ozone, chlorine activation, PSC surface area density and chemical ozone loss from the FinROSE simulation, and also the total ozone from the Ozone Monitoring Instrument (OMI) satellite instrument. It can be seen in the two uppermost rows that there is too low total ozone level in FinROSE compared to OMI observations. However, the spatial distribution of ozone is good in FinROSE. The left-hand column shows results for the 1st of March, when only a little solar radiation had reached the polar vortex, but chlorine had already started to be activated in the vortex. Ozone concentration in the vortex is smaller than outside. Also PSCs are formed inside the polar vortex but only minor ozone loss have occurred. The middle column shows results for the 15th of March when the ozone loss had started in the polar vortex. Chlorine activation had already been reduced from its maximum value. The PSC surface area density is in the same range as in the left column. In the rightmost column (the 1st of April) the chlorine compounds have already partly returned to reservoir species, and chlorine activation no longer exceeded the 50% level. Total ozone (two top rows) had clearly decreased in the polar vortex. Also over the northern Finland PSCs and very low ozone values can be seen. The maps in the bottom row in Fig. 4.1 describe the chemical ozone loss. The blue area in the centre of the polar vortex shows the ozone loss in the beginning of April. Even more than 40% of the ozone had been depleted. Above Finland the ozone depletion was about 30–40%, which is a significant reduction (Karpechko et al., 2013).

Figure 5 in PAPER I shows the corresponding parameters in the year 2000 (15th Jan, 15th Feb and 1st Mar). The ozone depletion was then only about 20%, i.e. less severe than in spring 2011 (Figure 4.1). Also PAPER V presents similar results from the FinROSE simulations. From Fig. 4.1 and PAPER I and PAPER V it can be seen that the FinROSE-CTM is able to simulate ozone depletion in the northern hemisphere.

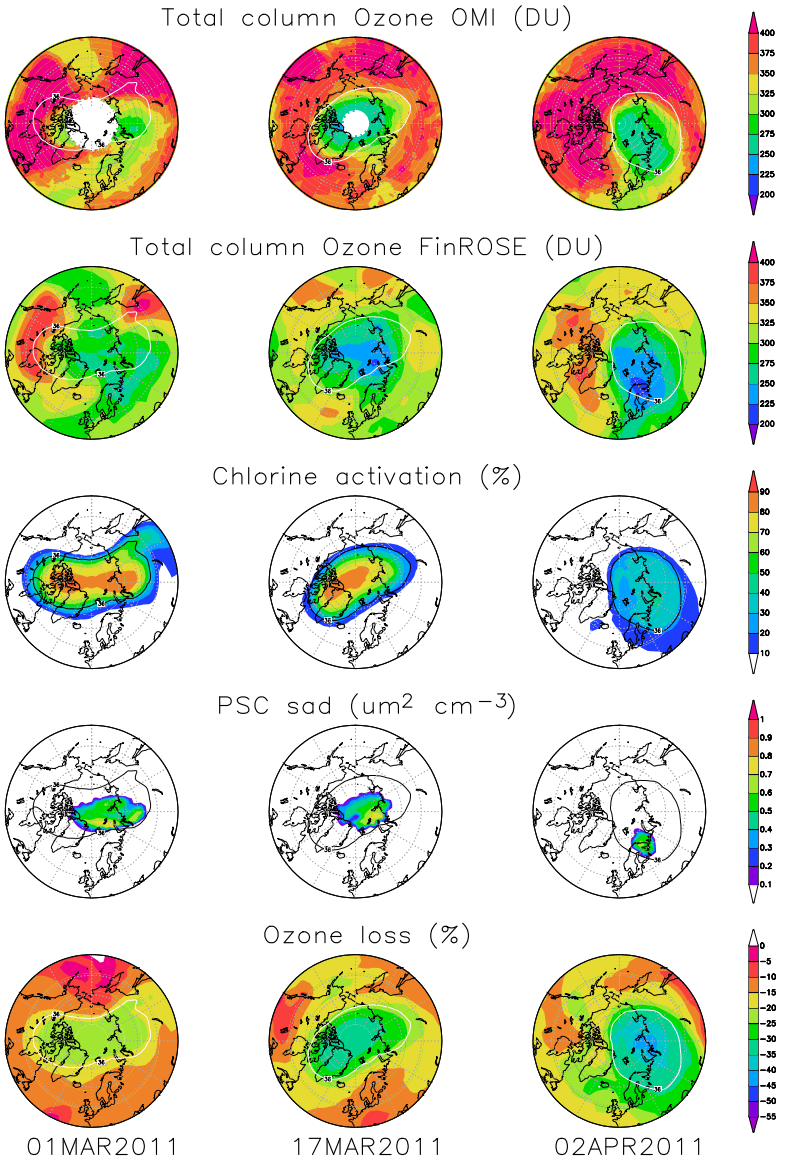


FIGURE 4.1. The evolution of ozone and key parameters for ozone loss during the 2011 northern hemispheric winter and spring shown as daily averages at the 475 K potential temperature level. Total column ozone (DU) from OMI in the uppermost row, total ozone from FinROSE in the second row, chlorine activation (%) in the third row, NAT and ICE PSC surface area density ($\mu$ m$^2$ cm$^3$) in the fourth row and ozone loss (%) in the bottom row. First column: 1st of March, second column: 16th of March and third column: 2nd of April in 2011. The 36 PVU isoline indicates the vortex edge at 475 K. (The figure is revised from Fig. 5 in PAPER I)

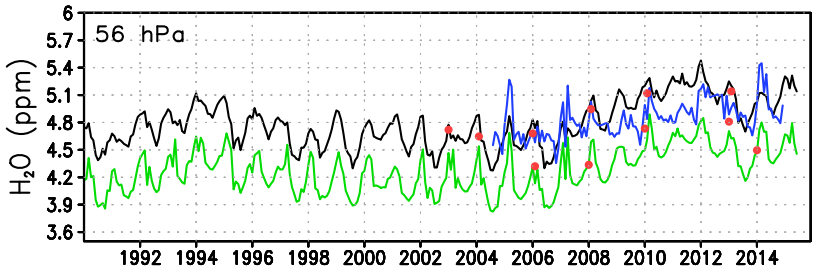


FIGURE 4.2. Water vapour of FinROSEn (black), ECMWF ERA-Interimin (green), MLS:n (blue) ja Sodankylä soundings (orange) at three levels. (The figure is revised from Fig. 4 from PAPER IV.)

Fig. 4.2 shows modelled water vapour, as well as the corresponding parameter from ECMWF ERA-Interim-data. Also MLS water vapour satellite observations and frost point hygrometer soundings from Sodanlylä are shown. The water vapour concentration of FinROSE is about 0.5 ppmv higher than in the ERA-Interim-data. FinROSE is close to the MLS data, although in FinROSE there is a positive trend in water vapour between 2009–2013, which is not seen from observations. A few soundings have been done every winter since 2003 at Sodankylä. The soundings are individual observations while the monthly means are shown for MLS, which may cause some discrepancy. Also the vertical grid of the model and MLS is much sparser than in the soundings, i.e. the modelled water vapour values represent a thicker layer than the sounding observations. FinROSE water vapour concentrations are closer to MLS than the values in ERA-Interim. This is likely due to the more complex chemistry scheme in FinROSE; ERA-Interim water vapour is only roughly parameterised based on the oxidation of $CH_4$ (Monge-Sanz et al., 2013).

## 4.2 DRIVER DATA

A chemistry transport model needs temperature, wind speed and direction as well as surface pressure fields pre-calculated. We have usually used the European Centre for Medium-Range Weather Forecasts ECMWF ERA-Interim meteorology and in the study described in PAPER II also the older re-analysis, ERA-40 (Thölix et al., 2010). In PAPER III it was pointed out that FinROSE-CTM can be run using climate model results as the driver data (Damski et al., 2007). However, the more common way is to

use re-analysis data sets. The driver data strongly affects the results of a CTM. The temperature is an important driver for the chemical reactions. The general circulation, which transports the gases from tropics to the polar areas can be even more important.

In PAPER II we tested the performance of the FinROSE chemistry transport model by using three different data sets from the ECMWF as the driver data. Simulations from 1990 to 2005 were done using winds and temperatures from the reanalysis data sets ERA-40 and ERA-Interim and from the ECMWF operational analysis. A good measure for the reliability of the driver data is the age-of-air, i.e the time an air parcel has spent in the stratosphere. When the age-of-air is too young, the Brewer–Dobson-circulation is too fast and the distribution of chemical compounds in the simulated atmosphere will be affected. For example ozone originates in the tropical region, and is transported with the BD-circulation to the polar areas. If the circulation is too fast, there may be too high amounts of ozone in the polar areas. A good quality of the driver data helps to give reliable distributions of the stratospheric species.

Waugh and Hall (2002) presented age-of-air estimates based on different measurements. Figure 4.3 shows a schematic for the annual mean of this age distribution between 15 and 35 km. It seen that the mean age-of-air reaches six years near the poles.

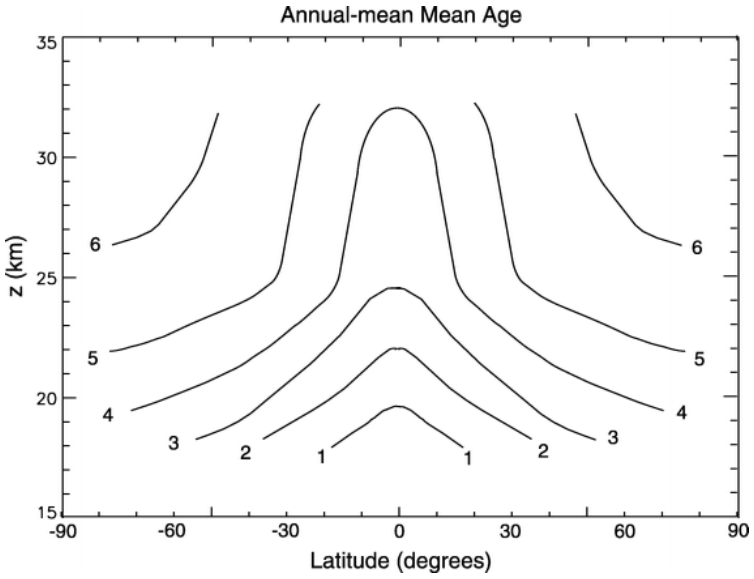


FIGURE 4.3. Annual mean of age-of-air based on observations. (Adapted from Waugh and Hall (2002)).

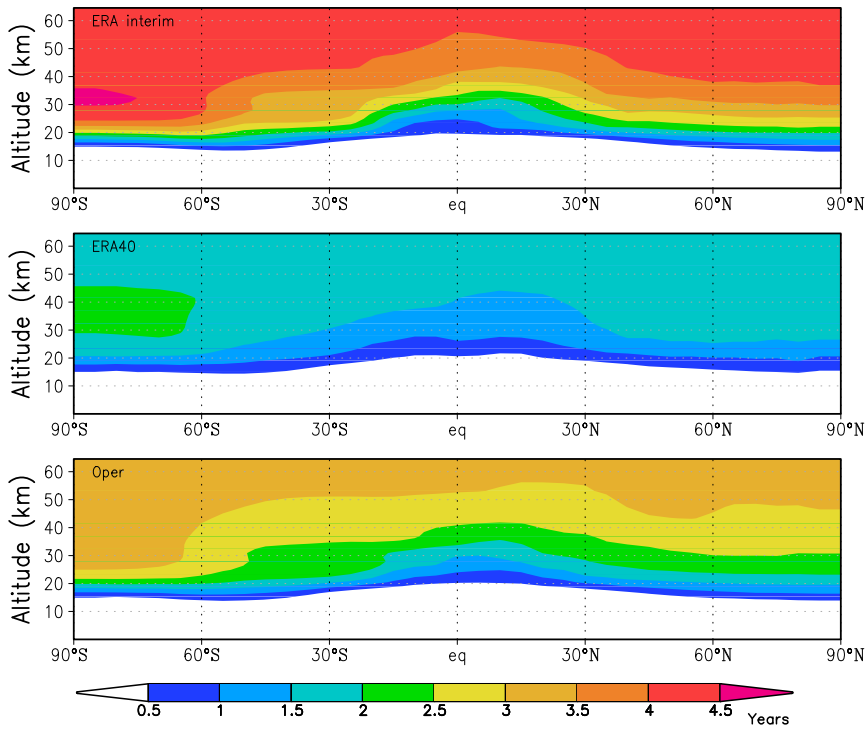


FIGURE 4.4. Vertical distribution of the monthly mean zonally averaged age-of-air (years) for July after 20 years of simulation in the FinROSE-CTM simulations using (a) ERA-Interim, (b) ERA-40 and (c) ECMWF operational data. (Figure 1 of PAPER II)

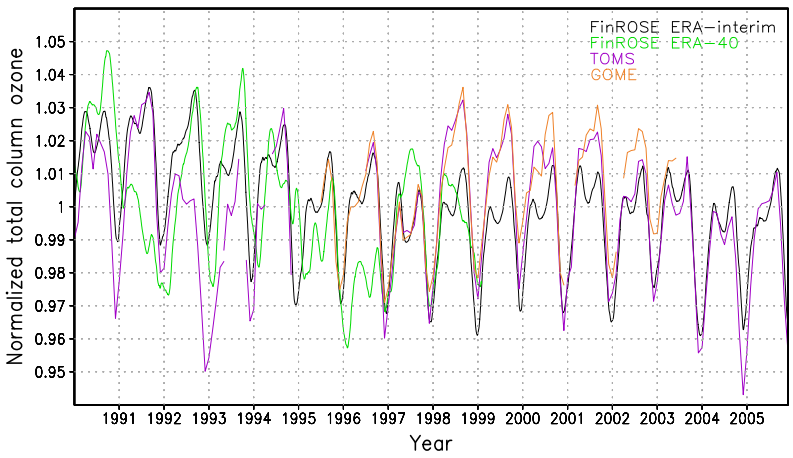


FIGURE 4.5. Normalized monthly mean global total column ozone ($60^\circ$ $S$ to $60^\circ$ $N$) time series from FinROSE-CTM simulations using ERA-Interim (black) and ERA-40 (green) analysis data, and from TOMS and OMI (purple) and GOME and SCIAMACHY (orange) observations. (Figure 2 of PAPER II)

Figure 4.4 shows the simulated age-of-air distribution after 20 years of simulations using the driver data sets described above. The oldest dataset ERA-40 resulted in a too strong BD-circulation with the maximum age-of-air of only about two years. The operational analysis gave improved results, more than a year older air, but the latest data set ERA-Interim resulted in a much more realistic upward transport. The age-of-air in the simulation using ERA-Interim data was about five years at maximum, which is still too young, but closer to the observations than in the other simulations, where earlier ECMWF re-analysis ERA-40 and the operational analysis data were used. Also the modelled ozone variability (shown in Fig. 4.5) is more realistic and showed better agreement with observations, when using the ERA-Interim. It was concluded that ERA-Interim is a useful dataset as a driver for CTMs.

## 4.3 LONG TERM TRENDS

In PAPER III the model was run using winds and temperatures from UMETRAC (Unified Model with Eulerian Transport and Chemistry) model (Austin and Butchart, 2003). Both past and ”future” years (1980–2019) were simulated, and also the concentrations and distributions for future ozone and other gases were calculated. The motivation

of this study was that the more sophisticated heterogeneous chemistry scheme of the FinROSE-CTM would provide an improved description of the ozone depletion than in the chemistry–climate model simulation. Also long reanalysis data sets were not yet available, and a CCM simulation gave a consistent data set for CTM simulations spanning several decades.

PAPER III shows ozone trends during the ozone loss years (1980–1999) and during the expected recovery period (2000–2019). Zonal mean decadal ozone trends for northern hemispheric spring months (March, April, May) from FinROSE and satellite measurements (TOMS and OMI) are shown in Fig. 4.6. The trends are calculated by applying a standard linear regression and the trend errors are based on the Student's T-test and the 95% significance level. The overall agreement between the model and observations is good. During the ozone loss period (lefthand panels) the ozone trend is negative in FinROSE at nearly all latitudes. It is also statistically significant elsewhere than in the tropics. Over the Arctic areas the spring trend in FinROSE is about -5%/decade. Near the poles both the modelled and observed trends are not significant while in the mid latitudes the trend is significant. Also the observed spring ozone trend is negative, but the error bars show that the trend is not significant over the Antarctica and in the tropics. The number of satellite measurements near the poles is quite limited. Therefore the observed trends near the poles are less reliable than in the middle latitudes and also the variability is larger.

During the recovery period (righthand panels), the spring ozone trend is instead mainly positive, but smaller than the negative trend during the loss period. FinROSE gives a positive trend of about 2–3%/decade over the southern latitudes and about 3-4%/decade over the northern latitudes. The trend is significant at the 95% confidence level elsewhere than in the tropics. The trends over the poles calculated from observations, which are now available for the years 2000–2017, are positive, however, they are not statistically significant. The asymmetry of the ozone trends between depletion and recovery period can likely be explained by the fact than ODS removal from the atmosphere is slower that ODS build up in the atmosphere. From the spring average point of view in the FinROSE simulation a small increasing trend of total ozone can be seen until 2019 in the south and in the north both from the observations and from the model simulation. Damski (2005) compared the ozone trends of FinROSE to the UMETRAC trends. From Fig. 4.19 and 4.20 of Damski (2005) it can be seen that the UMETRAC model slightly overestimates the spring trend compared to TOMS observations.

Fig. 4.7 shows the zonal mean ozone trends over northern hemispheric autumn months (September, October and November). During the ozone loss period there is a very large negative ozone trend, nearly -25%/decade, over the Antarctica in the FinROSE data. The autumn trend is negative also over nearly all other latitudes, but it is statistically significant only above Antarctica and the middle latitudes. Above the

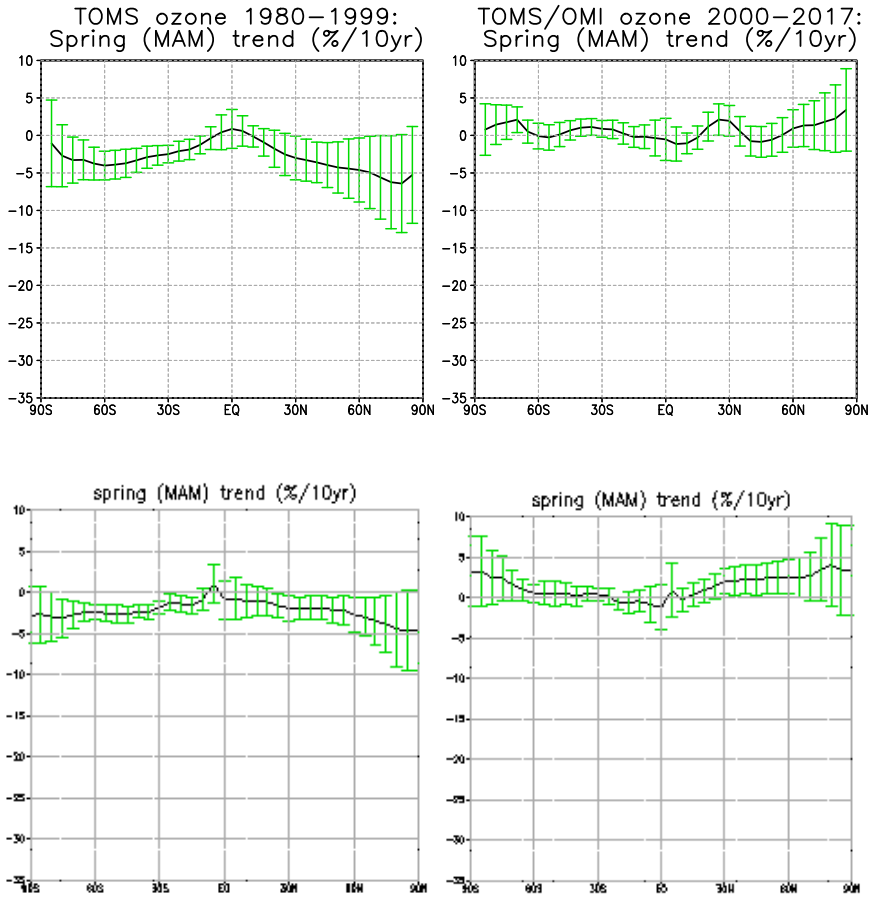


FIGURE 4.6. Zonally averaged total ozone trends over northern hemisphere spring months (March, April and May) [%/decade]. The errorbars indicate the 95% confidence intervals, calculated using the Students T-test. Upper row: trends calculated from observations. Lower row: Trends from the FinROSE simulation. Left panels show the ozone loss period and right panels the recovery period. (Figure modified from Fig. 10 of PAPER III)

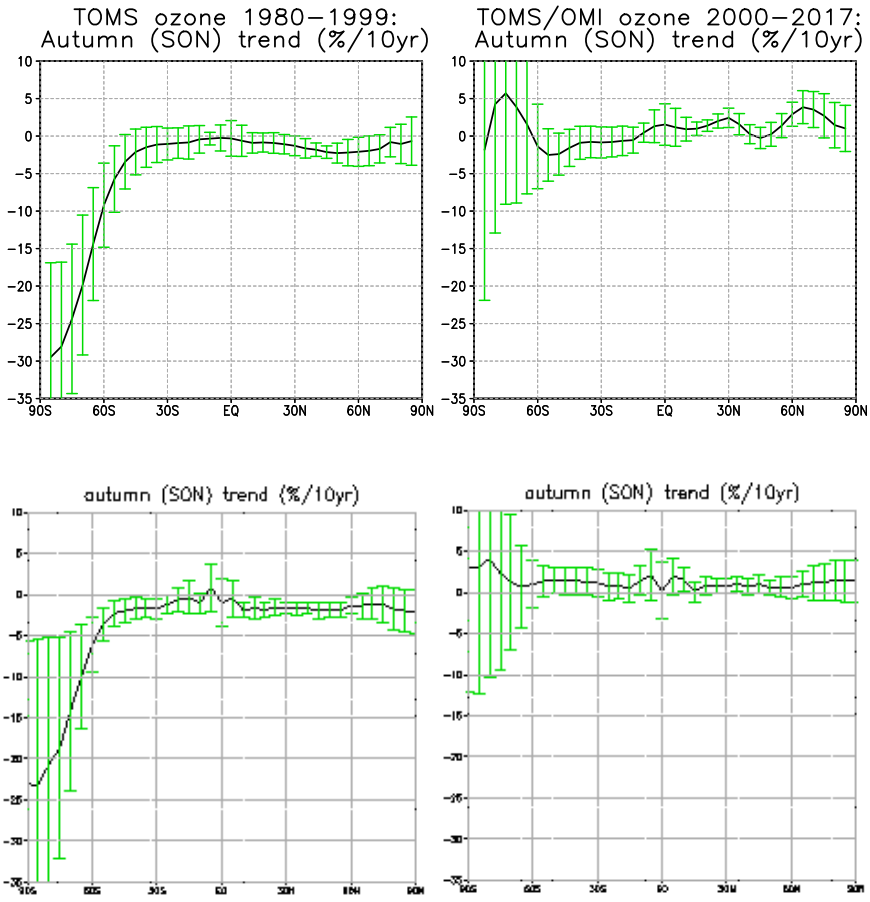


FIGURE 4.7. The same as Fig. 4.6 but over the northern hemisphere autumn months (September, October and November) [%/decade].

Arctic areas the autumn trend in FinROSE is about -2%/decade. The observed autumn ozone trends are also negative and above Antarctica even -30%/decade. During the recovery period the autumn ozone trend is mainly positive, but it is not significant in the model. No clear positive trend can be seen in the FinROSE data or observations in the recovery period. UMETRAC trends in Fig. 4.19 and 4.20 of Damski (2005) are clearly underestimated in the autumn during the ozone depletion period over the Antarctica, but during the recovery period the difference between the models is smaller. However, it can be seen that the ozone loss has not become worse after the 1990's and the recovery has started.

## 4.4 Water vapour changes in the Arctic stratosphere

The study in Paper IV evaluates the water vapour distribution and variability in the Arctic stratosphere. A FinROSE-CTM simulation was compared to observations, and the sources of SWV were studied. The study covers the years between 1990–2014. FinROSE-CTM was shown to be capable of simulating the stratospheric water vapour distribution and evolution in the Arctic. The water vapour distribution from FinROSE were compared to the ERA-Interim water vapour data. It was shown that the full stratospheric chemistry of a chemistry transport model produced a better water vapour distribution compared to the parameterised ERA-Interim water vapour, even though the ERA-Interim data was used as a tropospheric boundary condition. The dry bias of ERA-Interim data was alleviated and the FinROSE model gave results comparable to the MLS satellite measurements and Sodankylä frost point hygrometer measurements (see Fig. 4.2).

The main source of the stratospheric water vapour is the transport through the tropical tropopause. In FinROSE a chemically passive water vapour tracer was introduced for estimating the contribution of transported water vapour. SWV is also produced chemically from methane oxidation. The fraction of water vapour produced chemically was found to be smaller than the fraction brought by transport, but in the summertime at altitudes between 6 and 1 hPa (35–48 km) the fractions were almost as large. The decadal variability of water vapour and its sources between latitudes 70–90° N can be seen in Fig. 4.8 where anomalies of water vapour components are shown. The anomalies are calculated by subtracting the mean values for the period 1990–2014 for FinROSE and ERA-Interim and for the period 2004–2014 for MLS anomalies. The FinROSE simulation shows decadal variability in the Arctic water vapour with a magnitude of 0.8 ppmv. Both observations and the simulation show an increase in the water vapour concentration in the Arctic stratosphere after 2006, but around 2012 the concentration started to decrease. According to the simulation, the increase in water vapour is mostly explained by transport-related processes, while the photochemically produced

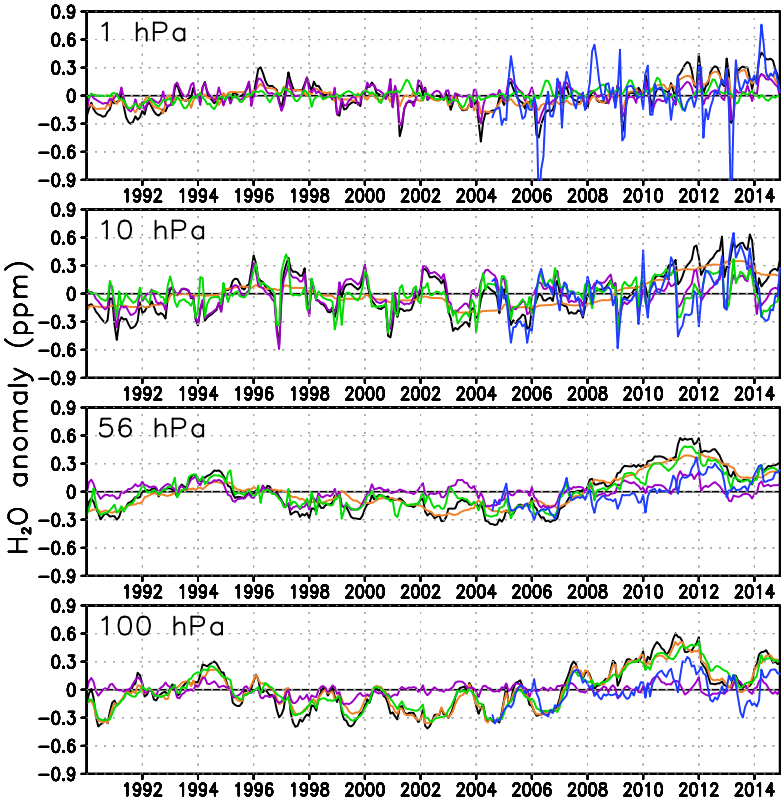


FIGURE 4.8. Anomalies of Water vapour (black), tracer describing transported water vapour (orange), tracer describing water produced by methane oxidation (purple) from FinROSE, and the water vapour anomaly from ECMWF ERA-Interim (green) as ppmv between 1990–2014 and the water vapour anomaly from MLS (blue) between 2004–2014. Anomalies are calculated over latitudes 70°–90° N at the levels of 1, 10, 56, and 100 hPa. (Modified from Fig. 5 of PAPER IV)

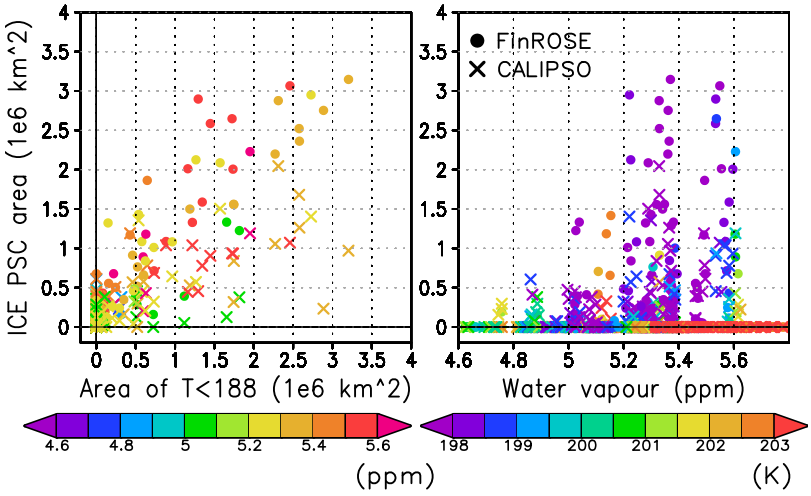


FIGURE 4.9. Panel (a): scatter plot of December–February ICE PSC area versus the area colder than 188 K in the Northern Hemisphere from FinROSE and CALIPSO at 56 hPa. The colour denotes the vortex mean water vapour content (ppmv). Panel (b): scatter plot of the December–February ice PSC area versus the vortex mean water vapour content (ppmv) from FinROSE and CALIPSO at 56 hPa. The colour denotes the vortex average temperature (K). FinROSE is shown with dots and CALIPSO is shown with crosses. (Fig. 8 of PAPER IV)

water vapour plays a relatively small role. A regression analysis suggests that both cold point temperature variability and QBO are important factors in the Arctic water vapour variability in the lower stratosphere.

Our results indicate that increased stratospheric water vapour concentration in the polar vortex has increased the ICE PSC occurrence after 2006. In the FinROSE simulation ICE PSCs occurred in the Arctic polar vortex in 12 out of 25 simulated winters, becoming more frequent in the latest years of the simulation. Figure 4.9 shows the relation of water vapour, temperature and ICE PSCs. The left panel shows the dependence of the ICE PSC area on the cold temperature area in December–February 2007–2014 at the 56 hPa level. Each datapoint denotes one winter day in the FinROSE simulation or in the observation by the Cloud-Aerosol-Lidar and Infrared Pathfinder Satellite Observations (CALIPSO). The colour of the mark shows the water vapour concentration averaged in the vortex. The cold area shows the area colder than 188 K. Figure 4.9, right panel, shows the dependence of ICE PSC on water vapour. If the temperatures were similar, the ICE PSC area would increase, when water vapour concentration in-

creases but in a dry vortex, no ICE PSCs form even at low temperatures. This is seen in both FinROSE and CALIPSO. An increase in SWV and a decrease in the stratospheric temperature enhances each other, and the volume of PSCs increases (Khosrawi et al., 2016). The temperature is the main factor controlling the ICE PSC formation, but the formation depends also on water vapour concentration. Higher concentrations produce larger areas of ICE PSC. The increase in water vapour within the vortex was about 0.8 ppmv after 2007 (see Fig. 4.8). That would have increased the ICE PSC areas even if the temperatures were the same, consistent with earlier estimations by Kirk-Davidoff et al. (1999).

Finally, we performed a case study of the extremely cold winter of 2009/2010. Figure 4.10 shows maps of temperature from ERA-Interim, the water vapour concentration and ICE PSC from FinROSE and ICE PSC from the CALIPSO satellite instrument from the Arctic polar area at the 35 hPa (24 km) level. The dates in the Figure were chosen according to the Sodankylä sounding dates between 17 and 23 January 2010. The polar vortex area is marked with a black line in the maps and is defined as modified PV $> 36$. The temperature in the vortex (1st row) was very low at this time period, minimum temperatures were even below 188 K. The water vapour concentration of FinROSE (2nd row) is the highest at the vortex boundary and the lowest in the middle of the vortex. Areas with very cold temperatures correlate with very low water vapour content areas, because of the ICE PSC formation (3rd row) and dehydration, i.e. water vapour is condensed into ice particles and sedimented downwards. Figure 4.10 (4th row) also shows the ICE PSCs observed by CALIPSO. Due to CALIPSO's measurement technique, the observations appear to be sparse, and it can be seen that the grid boxes where CALIPSO observed ICE PSCs are scattered over larger areas compared to FinROSE simulations. The bottom row in Fig. 4.10 shows modelled frost point temperature profiles above Sodankylä from FinROSE and temperature profiles from ECMWF ERA-Interim analysis, frost point temperature calculated from MLS satellite water vapour measurements, and observed frost point temperature from Sodankylä soundings. Overall, FinROSE is able to simulate the frost point temperature quite well. The ECMWF ERA-Interim temperature is close to or below the frost point temperature during the analysed time period. Then the formation of ICE PSC can also be simulated in FinROSE. The water vapour concentration decreases about 1 to 1.5 ppmv from the median values due to dehydration. In summary, FinROSE was able to reproduce stratospheric water vapour, ICE PSC formation and the magnitude of the dehydration in good agreement with the observations during the record cold period in the winter of 2010.

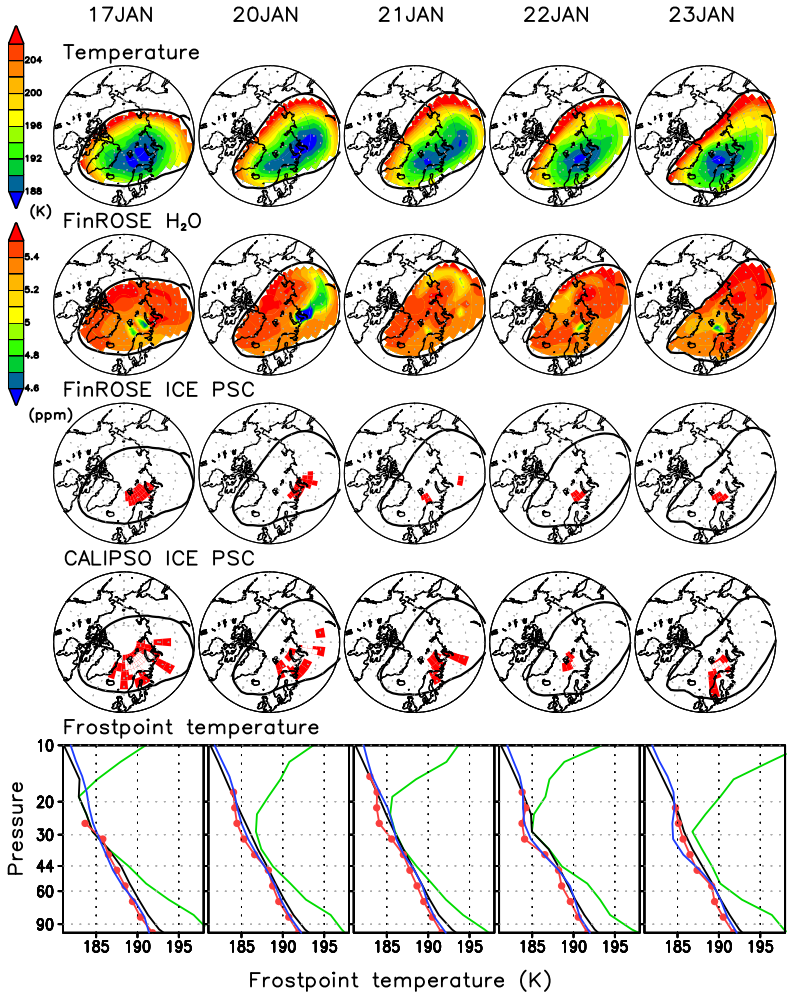


FIGURE 4.10. Upper four rows: temperature (K), water vapour (ppmv), and ICE PSC occurrence from FinROSE-CTM and ICE PSC occurrence from CALIPSO during winter 2010. The black contour marks polar vortex. All maps show the 35 hPa pressure level. Bottom row: ERA-Interim temperature (green) and frost point temperature from Sodankylä frost point hygrometer soundings (red dots), from MLS (blue), and from FinROSE (black). (Modified from Fig. 10 of PAPER IV)

## 4.5 Influence of water vapour to the Arctic ozone loss

Stratospheric water vapour influences the chemical ozone loss by controlling the PSC formation. There are large differences in the SWV between chemistry–climate models, because the models have difficulties in representing the amount of water vapour entering the stratosphere through the tropical tropopause. This has implications for the CCM's capability to simulate future stratospheric ozone losses in long term simulations. In this study we investigated the sensitivity of simulated Arctic ozone losses to the amount of water vapour entering the stratosphere using FinROSE-CTM. Three different simulations covering the years 2010–2016 were made. Here the results from the coldest winter 2010/11 and from a warmer winter 2013/14 are shown. The reference simulation was forced with ERA-Interim water vapour concentration in the tropical tropopause. In the Max-simulation, water vapour was increased by multiplying the ERA-Interim value by about 1.6 and in the Min-simulation the tropical tropopause concentration was about half of the ERA-Interim water vapour. The SWV values at the tropical tropopause approximately corresponded to the driest and wettest CCMVal-2 models (Gettleman et al., 2010). These modelled concentrations as well as MLS observations for 2014 can be seen in the left panel of Fig. 4.11. When forced by different SWV values at the tropical tropopause, FinROSE simulated different SWV concentrations through the whole stratosphere. The difference in the Arctic was very close to the differences prescribed at the tropical tropopause. The Arctic polar vortex water vapour concentrations in winter 2013/14 are shown in the right panel of Fig.4.11.

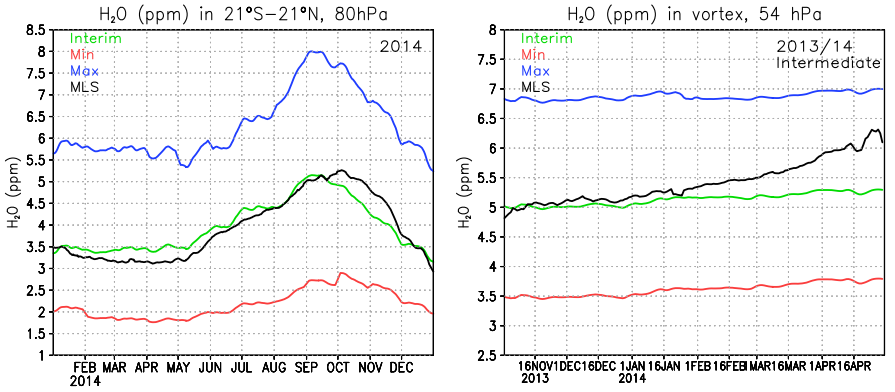


FIGURE 4.11. Left: Water vapour near the tropical tropopause in 2014. Right: Water vapour at 55 hPa within the Arctic polar vortex in winter 2013/14. The green line is the Interim simulation, the blue is Max, the red Min simulation. The black line shows the MLS observations. (Modified from Figs. 1 and 3 of PAPER V)

Consistent with expectation, the SWV amount strongly influences the amount of PCSs. Especially the area of air containing ICE PSC changes with changing SWV. Also the areas of NAT and STS PSCs depend on water vapour, but the effect is not so strong. We also see differences in chlorine partitioning between different SWV simulations. However, the temperature of the winter and the amount of PSCs affect the fraction of activated chlorine more.

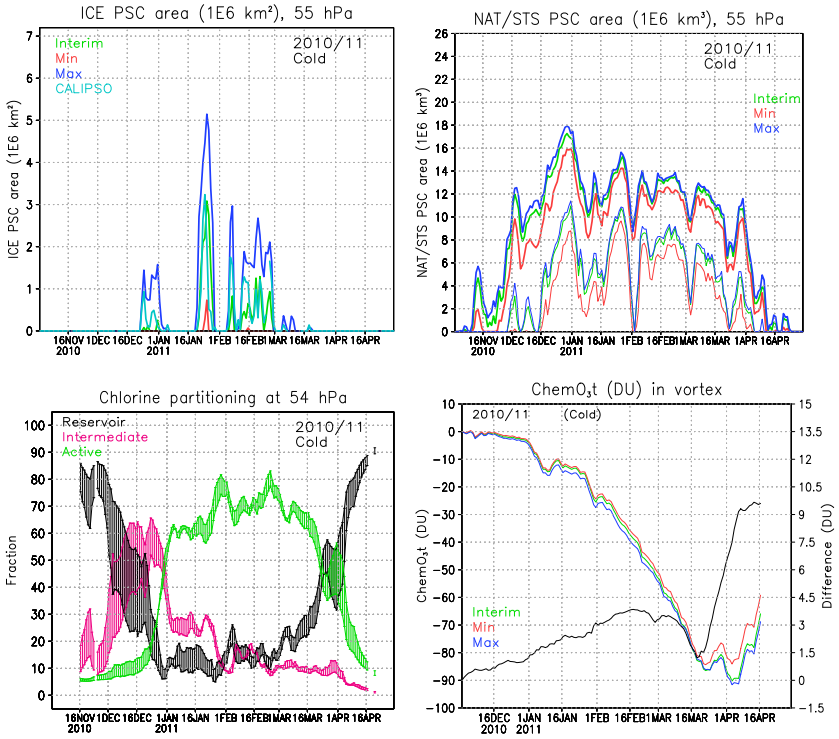


FIGURE 4.12. a) Area of ICE PSCs, b) area of NAT and STS PSCs, c) chlorine partitioning at 55 hPa and d) chemical ozone loss within the Arctic polar vortex in winter 2010/11. In panels a,b and d the green line is the Interim simulation, the red is Min and the blue is Max simulation. Panel c shows the difference between the Min and Max simulations. The black curve is the reservoir fraction, magenta is intermediate species and green is the fraction of activated chlorine. (Modified from Figs. 4–7 of PAPER V)

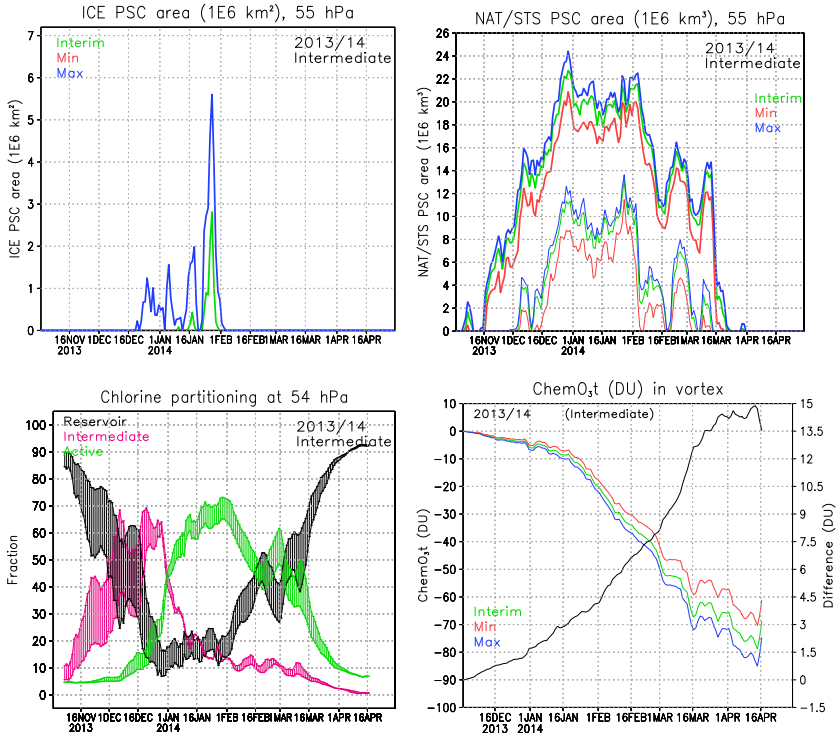


FIGURE 4.13. The same as Fig. 4.12, but in the winter of 2013/14. (Modified from Figs. 4–7 of PAPER V)

In Fig. 4.12 and 4.13 PSC areas, chlorine partitioning and corresponding ozone loss are shown for winters 2010/11 and 2013/14, respectively. the winter of 2010/11 was cold, and there were high amounts of ICE PSCs in the Interim simulation. In the Max simulation the ICE PSC area increased strongly compared to the Interim simulation and even in the Min simulation there were some ICE PSCs. In the case of NAT and STS PSCs the amount of water vapour was not so important, but also the area of NAT and STS increased with water vapour. Chlorine activation starts when the reservoir species start to transfer to intermediate ones. This happens at the same time with the growth of the NAT and STS area, i.e. at the beginning of November. At the beginning of January most of the chlorine is in active form. At the same time the chemical ozone loss starts in the Arctic polar vortex. The water vapour amount is important for the chlorine partitioning in December, but after that the difference between simulations is quite small when considering the activated chlorine. The difference between Min and

Max simulations (black line at the bottom right panel in Fig. 4.12) is about 10 DU. The difference between Min and Interim simulations is about 9 DU and between Interim and Max simulations only about 1 DU. The increase of water vapour did not significantly increase the ozone loss during winter 2010/11. In contrast winter 2013/14 (see Fig. 4.13) was only moderately cold. ICE PSCs were simulated, and their area increased with water vapour, but in the Min simulation there was almost no ICE PSC. The NAT and STS PSC areas were large in all runs and the areas correlates well with the chlorine activation. Water vapour amount changes the chlorine partitioning most before the chlorine activation, but also the fraction of activated chlorine depends on water vapour concentration. In the Max simulation a larger fraction of the chlorine is activated and correspondingly more ozone is destroyed than in the Man simulation. The difference in the chemical ozone loss between Min and Max simulations was as high as 15 DU in the winter of 2013/14.

From Figures 4.12 and 4.13 we can conclude that in cold winters the SWV has less control over the chlorine activation and ozone loss, because enough PSCs are formed even with low SWV to activate almost all the chlorine. In warmer winters the influence is larger, and the increase in ozone loss with water vapour is also larger. Although this change is not large in comparison to the total ozone loss, it does represent a source of uncertainty when analysing ozone depletion from CCM ensembles, for example for estimating future ozone recovery dates. In particular, it can be expected that a model with too much SWV would tend to simulate more ozone loss than a model with less SWV per given ODS amount, thus delaying simulated Arctic ozone recovery, assuming that vortex temperatures are similar between the models. It should also be noted that extra SWV would contribute to stratospheric cooling thus leading to a colder stratosphere and more PSCs and ozone loss. This effect was not taken into account in this study, because SWV concentrations did not affect temperatures in our CTM simulations.

# 5 CONCLUSIONS

The scientific goal of this study was to investigate the long term variability of stratospheric ozone and water vapour, the impact of water vapour on the ozone loss and the importance of the driver data. This work aims at showing for example the source responsible for the increase in stratospheric water vapour and the influence of tropical water vapour changes on Arctic water vapour and the ozone loss. Also, the usefulness of FinROSE-CTM in different kinds of stratospheric investigations was shown.

Although the chemistry of the ozone loss is well known and the success of the Montreal protocol has had a positive effect on the ozone layer, there are still questions to answer. Chlorine concentrations in the stratosphere have decreased after emission reductions following the Montreal protocol and the halogen loading in the stratosphere will further decrease during the next decades. Ozone depletion has decreased 20% during the southern hemispheric winter months from 2005 to 2016 (Strahan and Douglass, 2018). The increase in ozone levels is due to declining levels of chlorine coming from CFCs. But a clear decrease in the size of the ozone hole cannot yet be seen, because it is controlled mainly by the temperature, which varies a lot from year to year (Strahan and Douglass, 2018). However, Solomon et al. (2016) have already detected signs of ozone recovery in Antarctica in September because interannual variability is smaller in September than in October. Climate change warms the troposphere, but cools the stratosphere. The decreased chlorine loading would decrease the ozone loss, whereas the colder stratosphere would increase the PSCs, thus a smaller amount of chlorine could be sufficient to cause ozone loss in the polar vortex (e.g. Butler et al. (2016)). The stratospheric water vapour may increase due to increases in atmospheric methane and climate change, which would further cool the stratosphere and enhance PSC formation.

PAPER I and PAPER II describe the model, FinROSE-CTM, which is used in this thesis. The model can be run with different kinds of driver data sets and it is able to produce realistic distributions of ozone and water vapour, which are comparable to observations. Because FinROSE is cheap to run, it allows multiple simulations, at time scales from several days to multidecadal ones, which can be used for example in sensitivity studies. In addition to the studies explained in these thesis, the model has been used also in studies of Karpechko et al. (2013), Salmi et al. (2011) and Päivrinta et al. (2013). In particular PAPER II addresses the important question of the role of driver fields for simulating stratospheric trace gases.

Homogeneous and accurate meteorological data produces more realistic trace gas distributions. If the general circulation in the driver data is too fast, the age-of-air in the stratosphere becomes too young, and it is not possible to simulate correct atmospheric ozone and water vapour distributions. The use of ERA-Interim data improved the re-

sults of FinROSE-CTM remarkably, compared to earlier reanalysis data, and made carrying out the long simulations meaningful. The uncertainty in existing reanalysis data is large, so users should be careful in selecting the driving fields, choosing a unsuitable driver data set could result in an unreasonable tracer distributions.

When using climate model data as driver data, as in PAPER III, also future trace gas distributions can be investigated with a CTM. Then the processes of ozone loss can be studied in different climatological circumstances and also sensitivity tests can be performed by running several parallel simulations under different conditions. We ran FinROSE-CTM using UMETRAC CCM data and got results for the ozone depletion period (1980–1999) and for the ozone recovery period, after CFCs concentration started to decrease (2000–2019). The recovery period extends some years into the future. The decrease of ozone seems to stop and the amount of ozone is going to stay unchanged or start to increase during the first decades of the 2000's. Observations during 2000–2017 are available, so we were able to validate the recovery period ozone trend calculated with FinROSE with the observed trend. Both observed and simulated trends show small positive change in the ozone amounts near the poles at the local springtime. Thus it can be concluded that ozone losses will still be seen in the near future, although the ozone recovery has started.

The stratospheric water vapour distribution of FinROSE is closer to observations than the ERA-Interim one; i.e. the full chemistry of the FinROSE-CTM gives additional value compared to the parameterised ERA-Interim water vapour (Monge-Sanz et al., 2013). In PAPER IV the water vapour distribution in the stratosphere was studied. The use of a special water vapour tracer showed that the main source of the stratospheric water vapour is transport, while the chemically produced water vapour contributes a smaller fraction. The novel findings in PAPER IV were that the stratospheric water vapour concentration in the polar vortex has increased and thus also the ICE PSC occurrence have increased after 2006.

In PAPER V the effect of water vapour on the ozone loss was studied. Water vapour is transported from the tropics to the polar stratospheric areas, and there it affects the PSC formation and therefore the ozone loss. In this study the effect of different tropical water vapour concentrations on the Arctic ozone loss was investigated and the quantified impact of tropical WV on Arctic ozone losses is the main result. If the winter is very cold in the Arctic polar vortex, additional water vapour does not increase the ozone loss much, because a large fraction of chlorine is already activated. During intermediately cold winters the concentration of water vapour affects the ozone loss more.

In the future ozone depletion can also occur in the Arctic stratosphere. The amount of water vapour is one of the most significant factors in the development of ozone loss. In the climate models the accurate description of both ozone and water vapour is important, because their amount has an effect on the whole climate. CTMs will be

useful tools for case studies and investigation of some atmospheric phenomena also in the future. FinROSE could be used for those purposes, or for testing new chemistry schemes before implementing them in a CCM. The chemistry of FinROSE could also be used as a chemistry routine in CCMs.

# BIBLIOGRAPHY

Austin, J., and Butchart, N.: Coupled chemistry–climate model simulations for the period 1980 to 2020: Ozone depletion and the start of ozone recovery. Q. J. Roy. Meteorol. Soc., 129, 3225–3249, 2003.

Brewer, A. W.: Evidence for a world circulation provided by the measurements of helium and water vapor distribution in the stratosphere, Q. J. Roy. Meteor. Soc., 75, 351–363, 1949.

Butchart, N.: The Brewer–Dobson circulation, Rev. Geophys. 52, 157–184, 2014.

Butler et al.: Diverse policy implications for future ozone and surface UV in a changing climate, Environ. Res. Lett., 11, 2016.

Carslaw, K.S., Luo, B.P., Clegg, S.L., Peter, T., Brimblecombe, P., and Crutzen, P.J.: Stratospheric aerosol growth and HNO3 gas phase depletion from coupled HNO3 and water uptake by liquid particles, Geophys. Res. Lett., 21, 2479–2482, 1994.

Chapman, S.: A theory of upper atmospheric ozone. Mem. R. Meteorol. Soc., 3, 103–125, 1930.

Chipperfield, M. P., Dhomse, S. S., Feng, W., McKenzie, R. L., Velders, G. J. M., and Pyle, J. A.: Quantifying the ozone and ultraviolet benefits already achieved by the Montreal Protocol, Nat. Commun., 6, 7233, doi:10.1038/ncomms8233, 2015.

Chipperfield, M., Bekki, S., Dhomse, S., Harris, N., Hassler, B., Hossaini, R., Steinbrecht, W., Thiéblemont, R., and Weber, M.: Detecting recovery of the stratospheric ozone layer, Nature, 549, 211-218, doi:10.1038/nature23681, 2017.

Colella, P. and Woodward, P. R.: The Piecewise Parabolic Method (PPM) for GasDynamical Simulations, J. Comput. Phys., 54, 174–201, 1984.

Damski J.: A chemistry-transport model simulation of the stratospheric ozone for 1980 to 2019. Ph.D. thesis, University of Helsinki, 2005.

Damski, J., Thölix, L., Backman, L., Taalas, P., and Kulmala, M.: FinROSE – middle atmospheric chemistry and transport model, Boreal Environ. Res., 12, 535–550, 2007.

Damski, J., Thölix, L., Backman, L., Kaurola, J., Taalas, P., Austin, J., Butchart, N., Kulmala, M.: A chemistry–transport model simulation of middle atmospheric ozone from 1980 to 2019 using coupled chemistry GCM winds and temperatures, Atmos. Chem. Phys., 7, 2165–2181, 2007.

Dee, D. P., Uppala, S. M., Simmons, A. J., Berrisford, P., Poli, P., Kobayashi, S., Andrae, U., Balmaseda, M. A., Balsamo, G., Bauer, P., Bechtold, P., Beljaars, A. C. M., van de Berg, L., Bidlot, J., Bormann, N., Delsol, C., Dragani, R., Fuentes, M., Geer, A. J., Haimberger, L., Healy, S. B., Hersbach, H., Holm, E. V., Isaksen, L., Kallberg, P., Kohler, M., Matricardi, M., McNally, A. P., Monge-Sanz, B. M., Morcrette, J.-J., Park, B.-K., Peubey, C., de Rosnay, P., Tavolato, C., Thepaut, J.-N., and Vitart, F.: The ERA-Interim reanalysis: configuration and performance of the data assimilation system, Q. J. Roy. Meteorol. Soc., 137, 553–597, 2011.

Dvortsov, V. L., and Solomon, S.: Response of the stratospheric temperatures and ozone to past and future increases in stratospheric humidity, J. Geophys. Res., 106, 7505–7514, 2001.

Eyring, V. et al.: Long-term ozone changes and associated climate impacts in CMIP5 simulations, J. Geophys. Res. Atmos., 118, 5029–5060, 2013.

Fahey, D.W., Gao, R.S., Carslaw, K.S., Kettleborough, J., Popp, P.J., Northway, M.J., Holecek, J.C., Ciciora, S.C., McLaughlin, R.J., Thompson, T.L., Winkler, R.H., Baumgardner, D.G., Gandrud, B., Wennberg, P.O., Dhaniyala, S., McKinley, K., Peter, T., Salawitch, R.J., Bui, T.P., Elkins, J.W., Webster, C.R., Atlas, E.L., Jost, H., Wilson, J.C., Herman, R.L., Kleinböhl, A., and von König, M.: The detection of large $HNO_3$-containing particles in the winter Arctic stratosphere, Science, 291, 1026–1031, 2001.

Fahey, D.W., and Hegglin, M.I. (Coordinating Lead Authors), Twenty Questions and Answers About the Ozone Layer: 2010 Update, Scientific Assessment of Ozone Depletion: 2010, 72 pp., World Meteorological Organization, Geneva, Switzerland, 2011. [Reprinted from Scientific Assessment of Ozone Depletion: 2010, Global Ozone Research and Monitoring Project-Report No. 52, 516 pp., World Meteorological Organization, Geneva, Switzerland, 2011.]

Farman, J., Gardiner, B., and Shanklin, J.: Large losses of total ozone in Antarctica reveal seasonal ClOx/NOx interaction Nature, 315, 6016, 207–210, DOI: 10.1038/315207a0, 1985.

Fleming, E. L., Jackman, C. H., Stolarski, R. S. and Douglass, A. R.: A model study of the impact of source gas changes on the stratosphere for 1850–2100, Atmos. Chem. Phys., 11, 8515–8541, 2011.

Gettelman, A., Hegglin, M. I., Son, S. W., Kim, J., Fujiwara, M., Birner, T., Kremser, S., Rex, M., Añel, J. A., Akiyoshi, H., Austin, J., Bekki, S., Braesike, P., Brühl, C., Butchart, N., Chipperfield, M., Dameris, M., Dhomse, S., Garny, H., Hardiman, S.

C., Jöckel, P., Kinnison, D. E., Lamarque, J. F., Mancini, E., Marchand, M., Michou, M., Morgenstern, O., Pawson, S., Pitari, G., Plummer, D., Pyle, J. A., Rozanov, E., Scinocca, J., Shepherd, T. G., Shibata, K., Smale, D., Teyssèdre, H., and Tian, W.: Multimodel assessment of the upper troposphere and lower stratosphere: Tropics and global trends, J. Geophys. Res., 115, D00M08, doi:10.1029/2009JD013638, 2010.

Karpechko, A.Yu., Backman, L., Thölix, L., Ialongo, I., Andersson, M., Fioletov, V., Heikkilä, A., Johnsen, B., Koskela, T., Kyrölä, E., Lakkala, K., Myhre, C. L., Rex, M., Sofieva, V.F., Tamminen, J. and Wohltmann, I.: The link between springtime total ozone and summer UV radiation in Northern Hemisphere extratropics, J. Geophys. Res. Atmos., 118, 8649–8661, 2013.

Khosrawi, F., Urban, J., Lossow, S., Stiller, G., Weigel, K., Braesicke, P., Pitts, M. C., Rozanov, A., Burrows, J. P., and Murtagh, D.: Sensitivity of polar stratospheric cloud formation to changes in water vapour and temperature, Atmos. Chem. Phys., 16, 101–121, 2016.

Khosrawi, F., Kirner, O., Sinnhuber, B.-M., Johansson, S., Höpfner, M., Santee, M. L., Froidevaux, L., Ungermann, J., Ruhnke, R., Woiwode, W., Oelhaf, H., and Braesicke, P.: Denitrification, dehydration and ozone loss during the 2015/2016 Arctic winter, Atmos. Chem. Phys., 17, 12893–12910, https://doi.org/10.5194/acp-17-12893-2017, 2017.

Kirk-Davidoff, D. B., Anderson, J. G., Hintsa, E. J., and Keith, D. W.: The effect of climate change on ozone depletion through changes in stratospheric water vapour, Nature, 402, 399–401, 1999.

Kylling, A., Stamnes, K., and Tsay, S.-C.: A reliable and efficient two-stream algorithm for radiative transfer; Documentation of accuracy in realistic layered media, J. Atmos. Chem., 21, 115-150, 1995.

Lin, S.-J. and Rood, R. B.: Multidimensional flux-form semi-lagrangian transport schemes, Mon. Weather Rev., 124, 2046–2070, 1996.

Livesey, N. J., Santee, M. L., and Manney, G. L.: A Match-based approach to the estimation of polar stratospheric ozone loss using Aura Microwave Limb Sounder observations, Atmos. Chem. Phys., 15, 9945–9963, doi:10.5194/acp-15-9945-2015, 2015.

Manney, G. L., Santee, M. L., Rex, M., Livesey, N. L., Pitts, M. C., Veefkind, P., Nash, E. R., Woltmann, I., Lehmann, R., Froidevaux, L., Poole, L. R., Schoeberl, M. R., Haffner, D. P., Davies, J., Dorokhov, V., Gernandt, H., Johnson, B., Kivi, R., Kyrö,

E., Larsen, N., Levelt, P. F., Makshtas, A., McElroy, C. T., Nakajima, H., Concepcion Parrondo, M., Tarasick, D. W., von der Gathen, P., Walker, K. A., and Zinoviev, N. S.: Unprecedented Arctic ozone loss in 2011, Nature, 478, 469–475, 2011.

McElroy, M. B., Salawitch, R. J., Wofsy, S. C., and Logan, J. A.: Reductions of Antarctic ozone due to synergistic interactions of chlorine and bromine. Nature, 321, 759, 1986.

Molina, M.J., and Rowland, F.S.: Stratospheric sink for chlorofluoromethanes: chlorine atom-catalysed destruction of ozone, Nature, 249, 810–814, http://dx.doi.org/10.1038/249810a0, 1974.

Molina L.T and Molina M.J.: Production of Cl2O2 from the self-reaction of the ClO radical, J. Phys. Chem. 91, 433–436. 10.1021/j100286a035, 1987.

Monge-Sanz, B. M., Chipperfield, M. P., Untch, A., Morcrette, J.-J., Rap, A., and Simmons, A. J.: On the uses of a new linear scheme for stratospheric methane in global models: water source, transport tracer and radiative forcing, Atmos. Chem. Phys., 13, 9641–9660, 2013.

Montzka, S. A., Butler, J. H., Elkins, J. W., Thompson, T. M., Clarke, A. D., and Lock, L. T.: Present and future trends in the atmospheric burden of ozone-depleting halogens Nature, 398, 690–694, 1999.

Müller, R., Grooß, J.-U., Lemmen, C., Heinze, D., Dameris, M., and Bodeker, G.: Simple measures of ozone depletion in the polar stratosphere, Atmos. Chem. Phys., 8, 251–264, https://doi.org/10.5194/acp-8-251-2008, 2008.

NASA. Studying Earth's Environment From Space. June 2000. (Materials accessed during March 2018) http://www.ccpo.odu.edu/SEES/index.html.

Newman, P. A., Daniel, J. S., Waugh, D. W., and Nash, E. R.: A new formulation of equivalent effective stratospheric chlorine (EESC), Atmos. Chem. Phys., 7, 4537-4552, https://doi.org/10.5194/acp-7-4537-2007, 2007.

Päivrinta, S.-M., Seppälä, A., Andersson, M. E., Verronen, P. T., Thölix, L., and Kyröl, E.: Observed effects of solar proton events and sudden stratospheric warmings on odd nitrogen and ozone in the polar middle atmosphere. J. Geophys. Res., 118, 6837–6848. https://doi.org/10.1002/jgrd.50486, 2013.

Prinn, R. G., Weiss, R. F., Fraser, P. J., Simmonds, P. G., Cunnold, D. M., Alyea, F. N., O'Doherty, S., Salameh, P., Miller, B. R., Huang, J., Wang, R. H. J., Hartley, D. E., Harth, C., Steele, L. P., Sturrock, G., Midgley, P. M., and McCul-

loch, A.: A history of chemically and radiatively important gases in air deduced from ALE/GAGE/AGAGE, J. Geophys. Res., 105, 17751–17792, 2000.

Randel, W., Wu, F., Oltmans, S., Rosenlof, K., and Nedoluha, G.: Interannual changes in stratospheric water vapor and correlations with tropical tropopause temperatures, J. Atmos. Sci., 61, 2133–2148, 2004.

Ravishankara, A. R., Daniel, J. S. and Portmann, R. W.: Nitrous Oxide (N2O): the dominant ozone-depleting substance emitted in the 21st century, Science, 326, 123–125, 2009.

Rex, M., Harris, N.R.P., von der Gathen, P., Lehmann, R., Braathen, G.O., Reimer, E., Beck, A., Chipperfield, M., Alfier, R., Allaart, M., OConnor, F., Dier, H., Dorokhov, V., Fast, H., Gil, M., Kyrö, E., Litynska, Z., Mikkelsen, I.S., Molyneux, M., Nakane, H., Notholt, J., Rummukainen, M., Viatte, P., and Wenger, J.: Prolonged stratospheric ozone loss in the 1995/96 Arctic winter, Nature, 389, 835–838, 1997.

Rex, M., Salawitch, R. J., Deckelmann, H., von der Gathen, P., Harris, N. R. P., Chipperfield, M. P., Naujokat, B., Reimer, E., Allaart, M., Andersen, S. B., Bevilacqua, R., Braathen, G. O., Claude, H., Davies, J., De Backer, H., Dier, H., Dorokhov, V., Fast, H., Gerding, M., Godin-Beekmann, S., Hoppel, K., Johnson, B., Kyrö, E., Litynska, Z., Moore, D., Nakane, H., Parrondo, M. C., Risley, A. D., Skrivankova, P., Stübi, R., Viatte, P., Yushkov, V., and Zerefos, C.: Arctic winter 2005: Implications for stratospheric ozone loss and climate change, Geophys. Res. Lett., 33, l23808, 2006.

Riese, M., Ploeger, F., Rap, A., Vogel, B., Konopka, P., Dameris, M., and Forster, P.: Impact of uncertainties in atmospheric mixing on simulated UTLS composition and related radiative effects, J. Geophys. Res., 117, D16305, doi:10.1029/2012JD017751, 2012.

Rose K. and Brasseur G.: A three-dimensional model of chemically active trace species in the middle atmosphere during disturbed winter conditions. J. Geophys.Res., 94, D13, 16387–16403, 1989.

Salmi, S.-M., Verronen, P. T., Thölix, L., Kyrölä, E., Backman, L., Karpechko, A. Yu., and Seppälä, A.: Mesosphere-to-stratosphere descent of odd nitrogen in February–March 2009 after sudden stratospheric warming event, Atmos. Chem. Phys., 11, 4645–4655, 2011.

Solomon, S., Garcia, R. R., Rowland, F. S., and Wuebbles, D. J.: On the depletion of Antarctic ozone, Nature, 321, 755–758, 1986.

Solomon, S.: Stratospheric ozone depletion: a review of concepts and history, Rev. Geophys., 37, 275–316, 1999.

Solomon, S., Haskins, J., Ivy, D., and Min, F.: Fundamental differences between Arctic and Antarctic ozone depletion, P. Natl. Acad. Sci. USA, 111, 6220–6225, 2014.

Solomon, S., Ivy, D., Kinnison, D., Mills, M., Neely III, R., and Schmidt A.,: Emergence of healing in the Antarctic ozone layer, Science, 353, 269–274, 10.1126/science.aae0061, 2016.

Stolarksi, R. S., Douglass, A. R., Oman, L. D. O. and Waugh, D.: Impact of future nitrous oxide and carbon dioxide emissions on the stratospheric ozone layer, Environ. Res. Lett., 10, 034011, 2015.

Strahan, S. E., and Douglass, A. R.: Decline in Antarctic ozone depletion and lower stratospheric chlorine determined from Aura Microwave Limb Sounder observations. Geophys. Res. Lett., 45, 382–390. https://doi.org/10.1002/2017GL074830, 2018.

Thölix, L., Backman, L., Ojanen, S.-M.: The effects of driver data on the performance of the FinROSE chemistry transport model, IJRS, 31, 6401–6408, 2010.

Thölix, L., Backman, L., Kivi, R., and Karpechko, A. Yu.: Variability of water vapour in the Arctic stratosphere, Atmos. Chem. Phys., 16, 4307–4321, 2016.

Thölix, Karpechko, A. Yu, L., Backman, L. and Kivi, R.: Linking the uncertainty in simulated arctic ozone losses to modelling of tropical stratospheric water vapour, Atmos. Chem. Phys. Discussion, 2018.

Waugh, D.W., and Hall, T.M.: Age of stratospheric air: Theory, observations, and models. Rev. Geophys., 40, 4, 1010, doi:10.1029/2000RG000101.

WMO (World Meteorological Organization) Scientific Assessment of Ozone Depletion: 2002, World Meteorological Organization, Global Ozone Research and Monitoring Project-Report No. 47, 498 pp., Geneva, Switzerland, 2003.

WMO (World Meteorological Organization), Scientific Assessment of Ozone Depletion: 2014, World Meteorological Organization, Global Ozone Research and Monitoring Project-Report No. 55, 416 pp., Geneva, Switzerland, 2014.

Wohltmann, I., Wegner, T., Müller, R., Lehmann, R., Rex, M., Manney, G. L., Santee, M. L., Bernath, P., Sumińska-Ebersoldt, O., Stroh, F., von Hobe, M., Volk, C. M., Hösen, E., Ravegnani, F., Ulanovsky, A., and Yushkov, V.: Uncertainties in modelling heterogeneous chemistry and Arctic ozone depletion in the winter 2009/2010, Atmos. Chem. Phys., 13, 3909–3929, doi:10.5194/acp-13-3909-2013, 2013.